POTENTIAL ADSORPTION MECHANISMS OF DIFFERENT BIO-WASTES FOR REMOVAL OF DIAZINON FROM AQUEOUS SOLUTION

SITHA SEAN

A Thesis is submitted to the Graduate School of Naresuan University
in Partial Fulfilment of the Requirements
of the Master of Engineering Degree in Environmental Engineering
September 2019

Thesis entitled "Potential adsorption mechanisms of different bio-wastes for removal of diazinon from aqueous solution"

by Mr. Sitha Sean

has been approved by the Graduate School as partial fulfillment of the requirements for the Master of Engineering in Environmental Engineering of Naresuan University

Oral Defense Committee

..... Chair

(Associate Professor Wanpen Wirojanagud, Ph.D.)

..... Advisor

(Assistant Professor Dondej Tungtakanpoung, Ph.D.)

..... Co – Advisor

(Associate Professor Puangrat Kajitvichyanukul, Ph.D.)

..... Internal Examiner

(Jirapat Ananpattarachai, Ph.D.)

Approved

.....

(Professor Paisarn Muneesawang, Ph.D.)

Dean of the Graduate School

5 SEP 2019

ACKNOWLEDGEMENTS

The thesis could not have been completed without the unconditional support and special help from my advisor, co-advisor, family, friends, and members of the Centre of Excellence on Environmental Research and Innovation Laboratory (CERI).

First of all, I would like to express my deep gratitude to Assistant Professor Dondej Tungtakanpoung, my research advisor, for his patient guidance, precious suggestions, consistent encouragement, and useful critique to help me accomplish this research.

I would like to express my sincere appreciation to Associate Professor Puangrat Kajitvichyanukul, my research co-advisor, for her valuable and constructive suggestions during the planning and development of this research. I would also like to give special thanks to all the thesis committee members for their valuable time and helpful comments.

I would like to take this opportunity to thank Associate Professor Wanpen Wirojanagud and Doctor Jirapat Ananpattarachai for giving good comments, advice, sharing their knowledge and supporting my thesis writing. I also wish to extend appreciation to the CERI laboratory, Department of Civil Engineering, Faculty of Engineering, Naresuan University for granting me the use of their research facilities.

Furthermore, I wish to gratefully acknowledge the financial support from the Royal Scholarship under Her Royal Highness Princess Maha Chakri Sirindhorn's Education Project for Cambodia. I would also like to thank the Naresuan University Writing Clinic for editing my work.

Finally, I would like to thank my family and friends for their endless love, support, help, and encouragement throughout my research.

Sitha Sean

Title	POTENTIAL ADSORPTION MECHANISMS OF DIFFERENT BIO-WASTES FOR REMOVAL OF DIAZINON FROM AQUEOUS SOLUTION
Author	Sitha Sean
Advisor	Assistant Professor Dondej Tungtakanpoung, Ph.D.
Co-Advisor	Associate Professor Puangrat Kajitvichyanukul, Ph.D.
Academic Paper	Thesis M. Eng. in Environmental Engineering, Naresuan University, 2019
Keywords	Bio-waste, Pesticide, Kinetics, Isotherm, and Mechanism

ABSTRACT

This study investigated the isotherms, kinetics, and mechanisms of three types of bio-wastes derived from agro-wastes including corn cob, bagasse, and coconut fibre. These three types of agro-wastes were collected at the northern of Thailand and synthesized as the potential adsorbents for diazinon subtraction from the aqueous solution. The adsorption capacity differentiates of each bio-wastes were illustrated. Bio-wastes were synthesized for 4 h at temperature 600 °C and were modified by hydrofluoric acid (HF) to enhance the specific area and porosity. The SEM, BET, FT-IR, and pHpzc were used to analyse the characteristic of bio-wastes. Experimental results showed the different BET specific surface area were ranged from 67.42 to 402.42 $m^2.g^{-1}$ of each bio-waste. Meanwhile, SEM showed that bio-wastes possessed intricate pore network comprising micropores and narrow mesopores. The pore volume disseminations in pore size of micropores (<2 nm) and narrow mesopores (2-20 nm) of bio-wastes in the range 16.88-21.24 % and 56.57-69.22 %, respectively. Solution pH at 4 carried out the highest removal efficiency of diazinon. Pseudo-second-order kinetic model and Langmuir isotherm model showed the best fit to the experimental adsorption data. The maximum adsorption capacities of bio-wastes were in ranged 8.60-15.83 $mg.g^{-1}$. The pore filling and chemical adsorption participated in the adsorption mechanisms of diazinon and bio-wastes.

LIST OF CONTENTS

LIST OF CONTENTS (CONT.)

LIST OF TABLES

Table **Page**

LIST OF FIGURES

Figure **Page**

LIST OF FIGURES (CONT.)

Figure **Page**

LIST OF FIGURES

Figure **Page**

ABBREVIATIONS

AC	=	Activated carbon
ADI	=	Acceptable Daily Intake
BET	=	Brunauer–Emmett–Teller
BW	=	Bio-waste
BG-BW	=	Bagasse bio-waste
Calc.	=	Calculation
Con.	=	Concentration
CC-BW	=	Corn cob bio-waste
CF-BW	=	Coconut fibre bio-waste
DI	=	Deionized
EPA	=	Environmental Protection Agency
Eq.	=	Equation
Exp.	=	Experiment
FAO	=	Food and Agriculture Organization of the United Nations
FT-IR	=	Fourier Transform Infrared Spectroscopy
FO	=	First Order kinetic
HCl	=	Hydrochloric acid
HF	=	Hydrofluoric acid
Hg	=	Mecury
H_2SO_4	=	Sulfuric acid
H_2O	=	Water
LD	=	Lethal Dose
M	=	Molar
µm	=	Micrometre
$mg.L^{-1}$	=	Milligram per litre
nm	=	Nanometre
PAH	=	Polycyclic aromatic hydrocarbons
pHpzc	=	Point of zero charge
PSO	=	Pseudo-second-order model

ABBREVIATIONS (CONT.)

PFO	=	Pseudo-first-order model
Q_{max}	=	Maximum of adsorption capacity
SEM	=	Scanning electron microscope
SO	=	Second order kinetic
SSA	=	Specific surface area
Tem.	=	Temperature
TVP	=	Total volume pore
UV-Vis	=	Ultraviolet-Visible
WHO	=	World Health Organization
w/v	=	Weight by volume
π–π EDA	=	π–π electron-donor-acceptor
Ref.	=	Reference

CHAPTER I

INTRODUCTION

Background and Research Motivation

Pesticides are organic chemicals purposely intended for increasing agricultural yield, soil productivity, product quality (1-4). Moreover, It is internationally used to prevent or control pests, diseases, weeds, and other plant pathogens in an effort to reduce or eliminate yield losses in the agricultural field (1-3, 5). Pesticides range from insecticides (i.e. insects,), rodents (i.e., rodenticides) and weeds (herbicides) to microorganisms (i.e., algicides, fungicides or bactericides)" (6). Because pesticides have many advantages such as large availability, low cost, and increased food production, the amount of pesticide consumption is increasing more and more in the agriculture sector. However, many pesticides used in agriculture are highly toxic both to the environment and to living organisms, especially when their application is uncontrolled (7).

Recently, the contamination of surface and ground water by pesticides has become a serious environmental problem due to the extensive application of these agrochemicals in crop farms, orchards, fields and forest lands (8). As a result of storm runoff, leaching events can cause pesticides to be mobilized from fields to water bodies (7). The surface runoff, wind erosion, deposition from aerial applications, industrial discharges are also the source of pesticide contamination (8). According to (9) found organic pesticide residues have been reported in drinking water, agricultural water, and groundwater. In addition, pesticides are able to release into water, soil, and air through runoff, leaching and spray drift (5). Exposure to pesticides occurs primarily through eating food and drinking water that is contaminated with pesticide residues, whereas substantial exposure can also occur in or around the home (5, 6). Due to their highly persistent properties, pesticides bioaccumulate in food, and water, and can present a risk to animal and human health (7). Moreover, pesticides are indeed toxic to humans not only at high doses, responsible for acute poisonings but even in low doses, as are mixtures of pesticides (10). However, long-term exposure may lead to an array of health effects

including cancer, neurodegenerative diseases, reproductive, and developmental toxicity, and respiratory effects (10).

Almost 40% of worldwide pesticides are organophosphorus compounds, which were utilized in huge quantities due to its inexpensive and high efficiency in pest removal (11). Organophosphorus pesticides, such as azinphos-methyl, diazinon, dichlorvos, malathion, and parathion, are extensively used in agricultural activities (12). However, organophosphate pesticides are extremely toxic and, like some nerve agents, inhibit neuromuscular enzymes that are essential for normal function in insects, humans and many other animals (7, 12).

Diazinon is a common insecticide used for insects such as cutworms, wireworms, and maggots. It was also used to counteract the pests that live in some fruit tree and vegetables, tobacco, forage and field crops. Furthermore, diazinon is used to control indoor pests such as cockroaches, ants, scorpions, and other insects (13, 14). This pesticide is capable to damage human health, as well as animals, and plants due to water consumption. Therefore, pesticides entering water sources would be considered a serious issue.

At present, there are various means of pesticide removal from water. These include physical (adsorption), chemical (O_3/UV, hydrolysis, Fenton, and photocatalyst), and enzymatic approaches (1, 15). Among these methods, adsorption is a popular method and widely used for the removal of pesticides, heavy metals, and dyes from water and soil (9, 16). The adsorption method is a simple design and incurs lower costs and therefore needs a lower cash outlay (17).

Bio-wastes are popular absorbent materials, utilized in the removal of pesticides from the aqueous environment. With high porosity and large surface area, ash contents, a mineral component, many functional groups and aromatic structure, bio-wastes can be effective absorbents of toxic contaminants (17-19). Many studies reported that bio-wastes are effective absorbents but with different efficiency regarding conditions such as pyrolysis conditions, synthesis conditions, porous structure, functional groups, mechanisms, etc. (20).

In this study, bio-waste material obtained from three types of agro-waste, including corn cob, bagasse, and coconut fibre. The bio-wastes were synthesized by a slow pyrolysis method under oxygen-limited conditions to become potential adsorbents

for diazinon removal in the aqueous solutions and compare the adsorption capacity of each bio-waste. Moreover, the adsorption was investigated in the batch adsorption system, including isotherm, kinetics, and mechanisms.

Research Objectives

Main objective:

To investigate bio-waste material obtained from three types of agro-waste, synthesized as potential adsorbents for diazinon removal in the aqueous solutions and compare the adsorption capacity of each bio-waste

Sub-objectives:

1. To examine adsorption isotherms and kinetics
2. To observe adsorption capacity and make a comparison
3. To define and examine mechanisms between bio-wastes and diazinon

Research Significance

The result of this study will show methods of bio-waste synthesis, the optimum pH, concentration, and contact time for diazinon removal. The adsorption isotherms, kinetics, and mechanisms are also illustrated in this study.

Research Scope

1. Bio-wastes were obtained from synthesizing corncob, coconut fibre, and bagasse collected in Thailand.
2. Bio-wastes were subject to pyrolysis at the same temperature and contact times under oxygen-limited conditions.
3. Bio-wastes were washed with HF acid
4. The surface morphology of bio-waste was checked by SEM, while BET was used to analyse the specific surface area, and the functional groups were analysed by FT-IR.
5. Adsorption method: mechanisms, isotherms, and kinetics
6. The pesticide used in this adsorption study is diazinon

CHAPTER II

LITERATURE REVIEW

Properties of Diazinon

The pesticide under investigation in this study, diazinon, has been used in agriculture as a nematicide and insecticide against soil insects and pests of fruit, vegetables, tobacco, forage, field crops, rangelands, and pasture. It is also used to keep greenhouses and mushroom houses free of flies. Diazinon is an organophosphorus pesticide, of moderate mammalian toxicity, which is active against a variety of agricultural and public health pests (3). It is readily absorbed by the gastrointestinal tract, through intact skin, and by inhalation. It is converted in vivo to the oxygen analogue diazixon, which then inhibits cholinesterase (3). The LD_{50} is 300-400 $mg.kg^{-1}$ for technical grade diazinon in rats (3). ADI is 0.002 $mg.kg^{-1}.day^{-1}$ (3).

1. Chemical and physical properties of Diazinon

Chemical structure of diazinon is shown in Figure 1. Characteristics of diazinon is presented in Table 1.

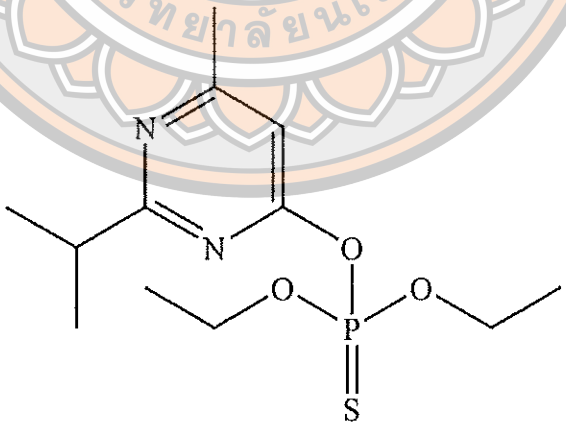

Figure 1 Chemical structure of diazinon

Table 1 The characteristics of diazinon (14)

Empirical formula	$C_{12}H_{21}N_2O_3PS$
Molecular weight	304.35 $g.mol^{-1}$
Chemical name	O,O-diethylO-(6-methyl-2-(1-methylethyl)-4-pyrimidinyl) phosphorothioate
Trade Names	Basudin, Cekuzinon, Dianon, Diazol, Dragon, Kayazinon, Knox Out, Neocidol, Spectracide, Terminator
Octanol/water partition coefficient	log Kow = 3.81
Volatility: Vapour pressure	9.01×10^{-5} mm Hg (25 °C)
Solubility	40 $mg.L^{-1}$ (20 °C)
pKa (ionization constant)	2.6

2. Use

Diazinon is used widely to kill insects via contact, stomach, and respiratory action. It is used to kill insects and their near relatives such as flying insects, crawling insects, mites, ticks, and spiders. It has been applied since 1950 to control sucking and chewing insects, and mites on fruit, vegetables, as well as forage and field crops. Diazinon was also used for general intention gardening and indoor pests to control cockroaches, silverfish, ants, and scorpions (14). Several investigators have found that levels of DDVP and diazinon residues were reduced by the pre-harvest intervals and/ or culinary applications, such as washing, peeling, and storage (3).

According to the solubility of diazinon is 40 $mg.L^{-1}$ at 20 °C, (4), it is found that water solubility of pesticides does not effluence to the quantity of pesticide reducing. The majority of pesticide residue appears to reside on the surface of produce where it is removed by the mechanical action of rinsing (4).

3. Transformation of Diazinon

3.1 Fate of Diazinon in the aquatic environment

Diazinon has stable properties in the water environment. The half-life of diazinon is around 6 months under neutral pH conditions at a temperature of 20 °C in the water. However, diazinon's half-life is 31 days at pH 5.0 and 136 days at pH 9.0. Diazinon has metabolism rapidly in acidic condition lead to diazinon is an exception herbicide, when it compares with other organophosphate pesticides (21).

3.2 Fate of Diazinon in the air environment

Diazinon is emitted into the atmosphere by the spraying of plants and using aerosols on animals. Moreover, diazinon readily enters the environment through water sources and the soil. It is a volatile substance which means that it readily evaporates into the air. In the air, the vapour and fine powder form of diazinon has a half-life of 4 hours. In addition, in the air, diazinon is converted quickly by UV rays. These reactions are enhanced under conditions of high temperature and humidity (21).

3.3 Fate of diazinon in the soil

In the soil, diazinon decomposed slowly where the half-life was around 6-12 weeks under neutral and sterile conditions. The half-life of the pesticide was around 2-7 weeks with bacteria. These figures can differ according to the properties of the soil including soil type and moisture content. The pesticide's metabolism is rapid in acidic pH and at high temperatures in the soil. Up to 50 % of diazinon or metabolites can be bond by soil components containing humic acids or other stable organic and mineral compounds (21).

4. Toxicity of diazinon

Diazinon can influence the body as it is absorbed through respiration, the eyes, the skin, or is swallowed. Diazinon is metabolized readily by mammals and is usually excreted through the urine. It is metabolized in vivo by four enzyme systems, which include mixed functions oxidases, hydrolases or phosphatases, glutathione dependent transferees, and non-specific exterases. In vivo animal studies have indicated that the production of diazoxon dydroxydiazinon, isohydroxydiazinon, and a propylenediazinon metabolite occurs in the body on exposure to diazinon. Diazinon does not bioaccumulate in tissues or organs. The mode of action of diazinon is the inhibition of the enzyme cholinesterase.

Diazinon is highly toxic to birds. The acute oral LD_{50} ($mg.Kg^{-1}$) for technical diazinon is 6.81 for turkeys; 40.7 for chickens; 14.7 for geese; 2.75 for goslings. The sub-acute dietary LC_{50} (ppm) for technical diazinon is 191 for mallard ducks; 245 for bobwhite quail; 244 for ring-necked pheasants and 47 for Japanese quail.

Properties of bio-waste

1. Bio-waste characterization

Bio-waste is a by-product of pyrolysis, gasification, torrefaction, and hydrothermal carbonization, which is made from biomasses such as agricultural crop residues, wood or waste at high temperature (300-900 °C) and under limited oxygen conditions (22). With high porosity, large surface areas, ash contents, a mineral component, many functional groups, and an aromatic structure, bio-wastes are treated as an effective absorbent in the removal of pollutants from aqueous solutions (17-19). Previous studies have demonstrated that bio-waste has a high specific surface area, heterogeneous surface properties, a microporous structure, the presence of different functional group compositions and resistance to decomposition and mineralization (19, 23).

The formation process of bio-waste requires less energy than in the production of activated carbon, but the porous structures are similar. Moreover, the cost of bio-waste processing is affordability compared to activated carbon due to the source material of bio-waste that comes from agricultural waste, which has low economic value. This is the main reason why bio-wastes have become popular as efficient absorbents. This suggests that bio-waste has economic value, can decrease the quantity of solid waste in the environment such as aggressive plants, impracticable growth reduction, and animal faecal matter, (24). Hence, the transformation of useless wastes to bio-wastes, (effective absorbents) helps in both waste management and environmental preservation as shown in Figure 2.

Previous studies have indicated that the properties and surface area of bio-wastes are very important in their ability to remove pollutants from the environment. The function of those properties enables bio-wastes to remove contaminants such as heavy metals, organic pollutants, and other pollutants like chemical waste from the environment. Of the studies of bio-wastes, 46 % focused on heavy metal extraction,

39 % examined organic pollutants, 15 % ammonium/nitrate and phosphate (NP), and 2 % for general pollutants (24). The adsorption characteristics of pollutants with bio-waste are shown in Table 2.

Table 2 Adsorption characteristics of pollutants with bio-waste (24)

Source	Pyrolytic Tem. (^{0}C)	Contact time	Pollutants	Qmax (mg/g)	Isotherm model	Kinetic model
Cattle manure	100	6 h	Al	-	Langmuir	-
Corn straw	600	2 h	Zn (II)	11.0	Langmuir	PSO
Hardwood	450	<5 s	Cu(II)	6.79	Langmuir	PSO
Eucalyptus	400	30 min	Methylene blue dye	2.06	Langmuir	PSO
Maize straw	300	1.5 h	Oxytetracycline	-	Freundlich	PSO
Palm bark	400	30 min	Methylene blue dye	2.66	Langmuir	PSO
Peanut shells	300	3 h	Trichloroethylene	12.12	Langmuir	-
Peanut shells	700	3 h	Trichloroethylene	32.02	Langmuir	-
Soybean stover	300	3 h	Trichloroethylene	12.48	Langmuir	-
Soybean stover	700	3 h	Trichloroethylene	31.74	Langmuir	-
Swine manure	400	1 h	Atrazine	14.79	-	PSO

Note: PSO: Pseudo-second-order model

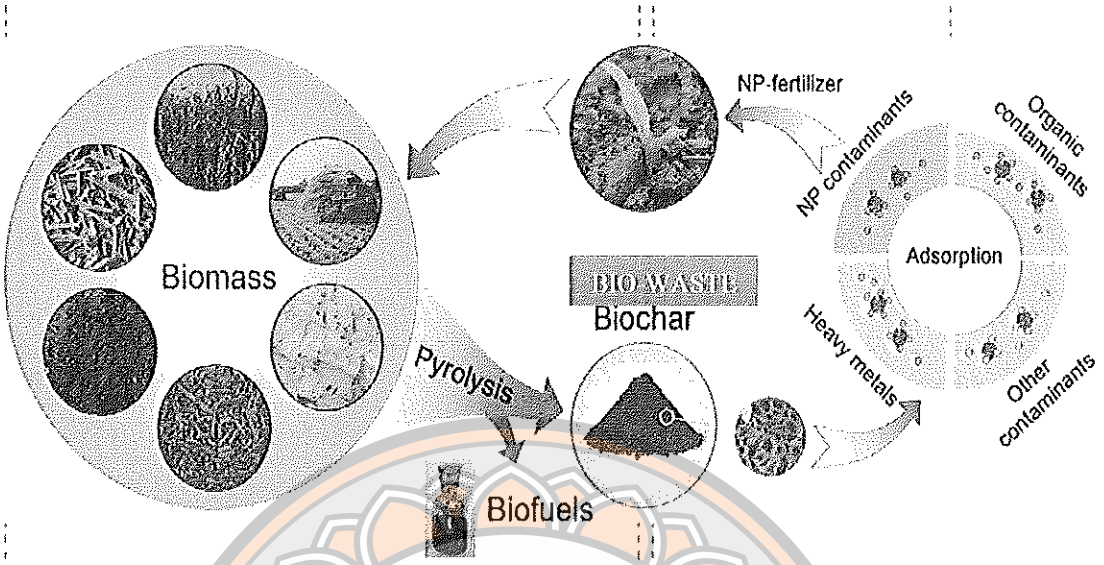

Figure 2 Benefits of bio-waste applied as an effective adsorbent for wastewater treatment (24)

For evaluating the removal efficiency of the contaminants by bio-wastes, the identification of the underlying mechanisms of the adsorption process is needed. According to (24), bio-waste adsorbs organic pollutants by means of various interactions. The adsorption mechanisms of organic pollutants by bio bio-waste is proposed in Figure 3. It is includes electrostatic interaction, hydrophobic effect, hydrogen bonding interaction, and a pore-filling mechanism.

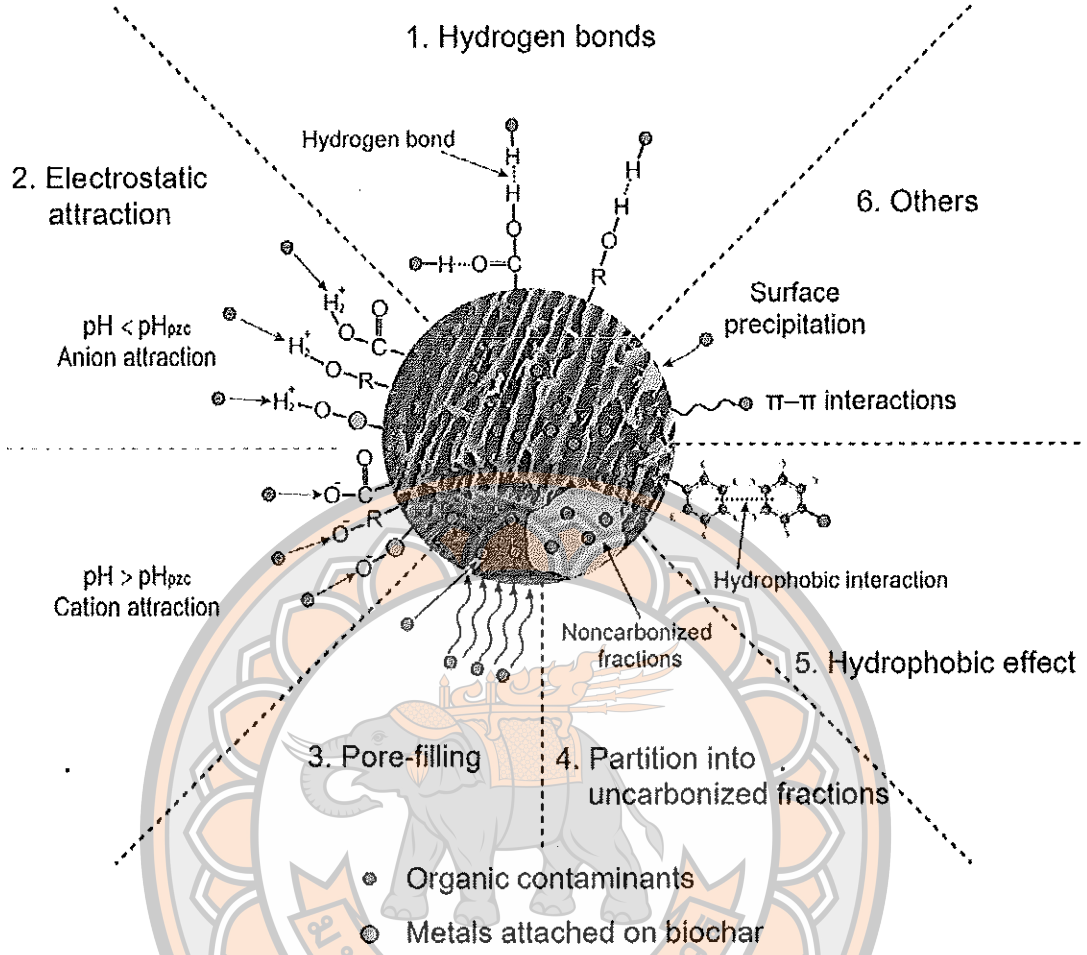

Figure 3 Adsorption mechanisms of organic pollutants (24)

A positive correlation between micropore volume and surface area suggests that pore size distribution is a key factor responsible for the increase in surface area in bio-waste. Bio-wastes produced from animal litter and solid waste feedstock exhibit lower surface areas compared to bio-wastes produced from crop residue and wood biomass, or even at higher pyrolysis temperatures (23). Major bio-waste characteristics relevant to specific environmental and agricultural applications are shown in Figure 4.

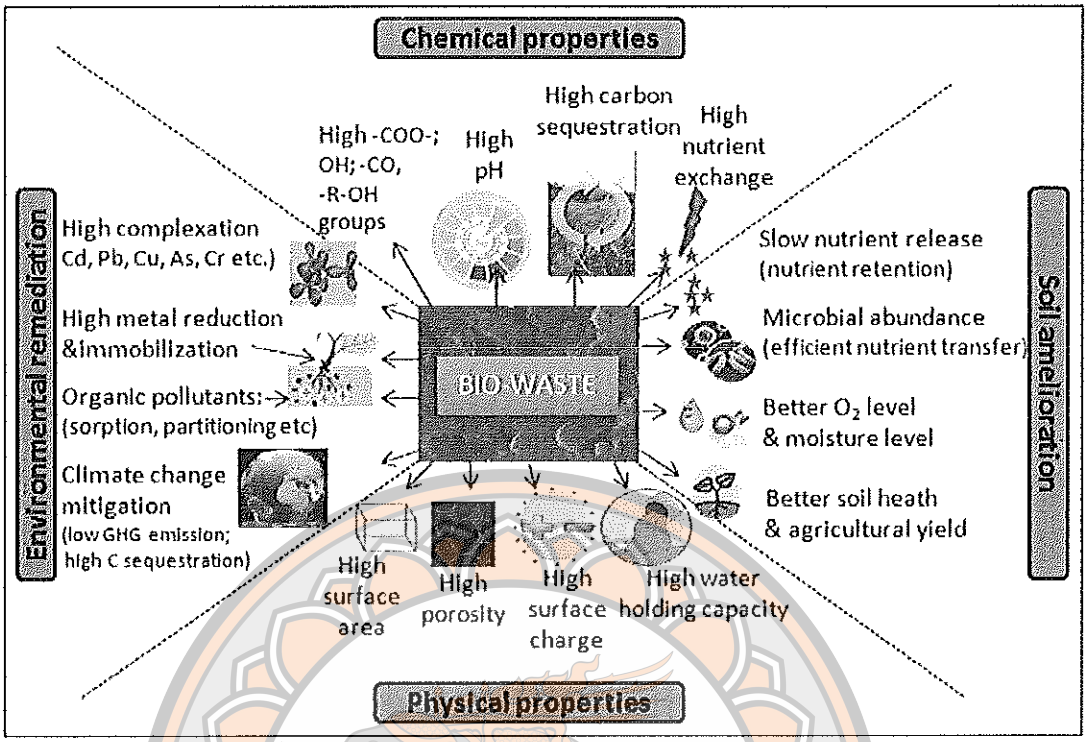

Figure 4 The specific environmental and agricultural applications of bio-waste (22)

2. Bio-waste synthesis

The pyrolysis conditions, gasification, torrefaction, and hydrothermal carbonization are the main thermochemical technologies for bio-waste production (22). Moreover, the pyrolysis conditions played an important role in bio-waste yield determination. There are two main pyrolysis conditions including slow pyrolysis and fast pyrolysis. The bio-waste yields synthesized from slow pyrolysis are higher than fast pyrolysis or gasification. The yields of 30 %, 12 %, and 10 %, of the bio-waste obtained from slow pyrolysis, fast pyrolysis, and gasification, respectively, performed at a longer residence time and at a moderate temperature (350–550 °C) in the absence of O_2 (20).

However, the surface areas and pore volumes of bio-waste commonly increase parallel with the temperatures and contact time (20). The result of (25) studied showed that the BET N_2 specific surface area of oak bio-waste increased from 2-225 $m^2.g^{-1}$ when increasing temperatures from 450 to 650 °C at 3 h. The specific surface area of pig manure bio-waste was also increased from 24 to 33 $m^2.g^{-1}$ when temperatures were increased from 350 to 700 °C at a contact time of 12 h (26). On the other hand, in

similar conditions, temperature and holding time, plant bio-wastes might have specific surface area higher than animal bio-waste (27). This is because of the quantity of inorganic and ash components in animal bio-waste is higher than plant bio-waste. Pyrolysis and gasification are thermochemical processes that produce bio-waste as a solid product, in addition to bio-oils and synthesis gas as shown in Figure 5.

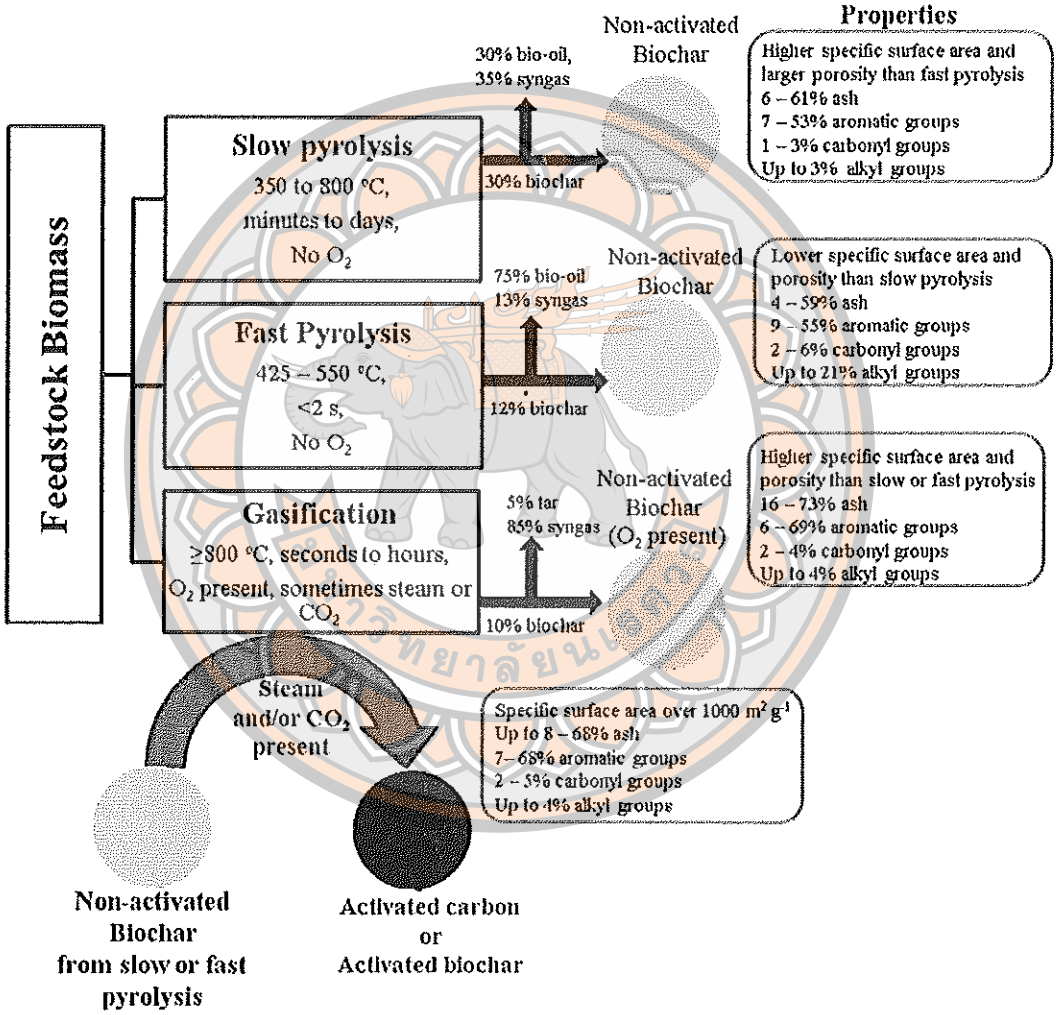

Figure 5 Characteristics of synthesis bio-waste under different pyrolysis conditions (20)

Under the slow pyrolysis conditions lower than 600 °C, the chemistry parent feedstock of bio-waste did not change. Nevertheless, when the temperature increases above 600 °C, it caused the aliphatic groups to change. For an instant, phenols and carboxylic acids can transform to neutral or fused basic aromatic groups. Pig manure bio-waste was produced at 620 °C for 12 hours, the NCH and N-C=O group were not found in raw manure. The polycyclic aromatic compounds that were formed include dioxins and furans in slow pyrolysis at 350 - 500 °C and the holding time was less than 1 hour (20).

Mechanism of bio-waste adsorption

Mechanisms of pesticide sorption on bio-waste are complicated, which consists of pore filling, hydrogen bonding, hydrophobic, electrostatic attraction, π-π electron donor-acceptor (π-π EDA) and partitioning into non-carbonized fraction (22). These mechanisms are shown in Figure 6. The sorption capacity of pesticide on bio-waste depends on both bio-waste properties and the functional group of the pesticide (23).

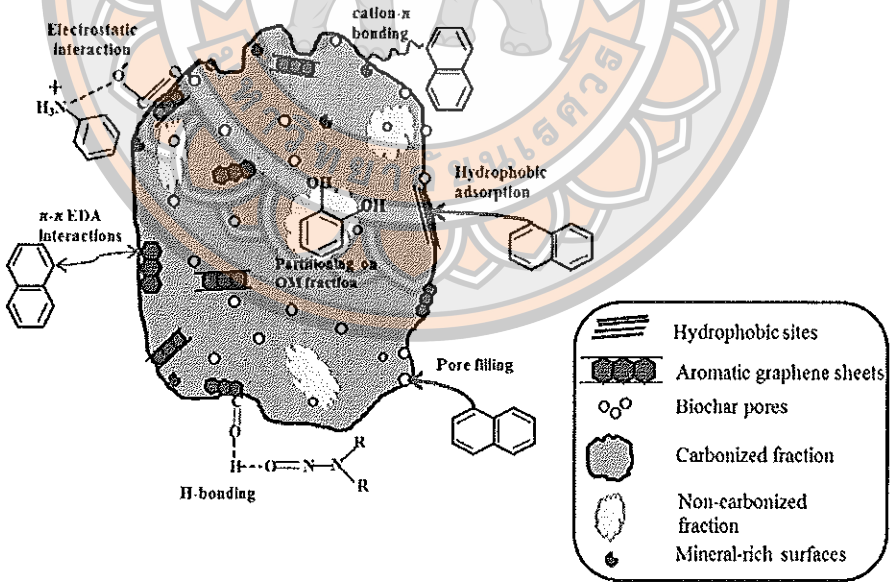

Figure 6 Characteristics of the mechanism of bio-waste adsorption (23)

1. Pore-filling

The pore network of bio-waste is similar to porous carbon, which was separated into three sizes. These types including micropores (<2 nm), mesopores (2-50 nm) and macropores (>50 nm). However, micropores and small mesopores (2-20 nm) are typically suggested to be present on the majority of bio-waste surfaces and plays the main role in the uptake of organic compounds. According to (20), the total micropore and mesopore volumes of bio-waste are the main functions in the pore-filling mechanism of organic adsorption. This mechanism was also reported by (26), where a lack of micropores in bio-waste produced at 350 °C, made the sorption capacity of atrazine and carbaryl lower. The pore-filling mechanism is dominant in the adsorption process where there are low pollutant concentrations in the solution or where there is a low volatile matter content of bio-waste.

The organic compound including both polar and non-polar can be adsorbed by pore filling depends on the bio-waste type (20).

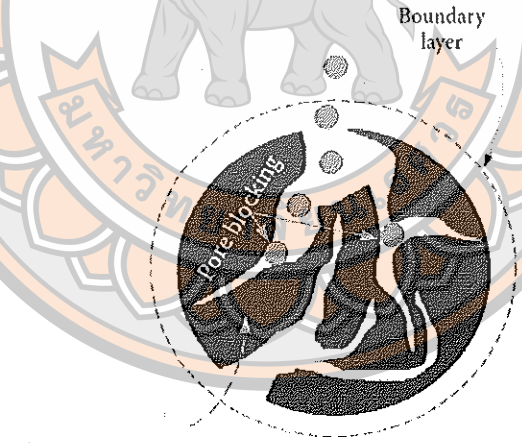

Figure 7 Pore-filling (28)

2. Hydrogen bonding

Hydrogen bonding (H-bonding) is a credible mechanism for the sorption of polar organic compounds on bio-wastes. Bio-wastes have plenty of polar groups on the surface such as –COOH, -OH, -CHO, -CO, which enhances the sorption capacity of polar pesticides on bio-wastes via H-bonding. The abundant polar groups on bio-wastes

facilitate water sorption and promote H-bonding between bio-wastes and organic adsorbates containing electronegative elements (29). For example, the sorption of dibutyl phthalate (DBT) by rice straw and swine manure bio-wastes was attributed to H-bonding between H-donor groups or water molecules on the bio-wastes and O-atoms on DBT's ester group (20). H-bonding of AN-O groups of NDMA with AC-O moieties in bamboo bio-waste was suggested to promote the removal of NDMA from aqueous solution onto bio-waste. Following (30), suggested that the sorption of glyphosate by rice husk-derived bio-wastes was attributed to H-bonding between surface phenolic and carboxylic groups of bio-wastes and H-atom or O-atoms on glyphosate's phosphates group. The polar organic groups on the surface of the bio-waste can participate in H-bonding. Many polar groups on bio-waste facilitate water sorption and impellent H-bonding between bio-waste and organic pollutants. The property of hydrogen bonding is shown in Figure 8.

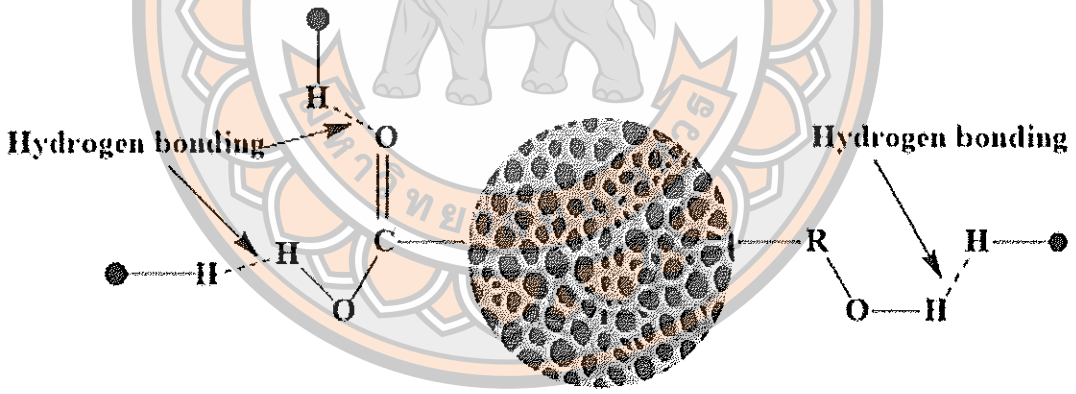

Figure 8 Hydrogen bonding

3. Hydrophobic interaction

Both partitioning and hydrophobic are the main factor in the hydrophobic interaction mechanism of organic compounds extraction by using bio-waste (20). Hydrophobic bio-waste with low surface oxidation is able to absorb hydrophobic organic compounds or neutral, and ionogenic organic. For example, the hydrophobic interaction mechanism occurred between hydrophobic C-F chain of Perfluorooctane

sulfonate and hydrophobic sites on maize straw and willow derived bio-wastes (20). The requirement of hydration energy of hydrophobic adsorption is lower than the partitioning adsorption.

The bio-waste becomes more hydrophobic when its surface contains the aliphatic and aromatic functional groups (31, 32). Consequently, it can adsorb hydrophobic pesticides by the hydrophobic adsorption mechanism which is shown in Figure 9.

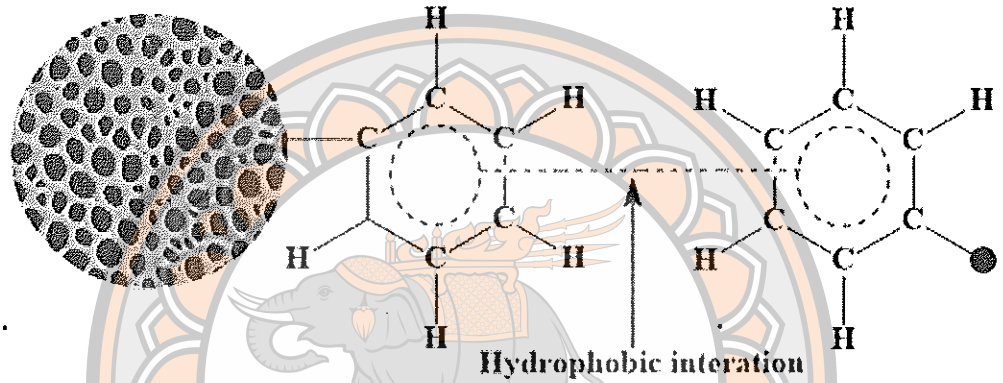

Figure 9 Hydrophobic interaction

4. π-π electron-donor-acceptor (π-π EDA)

π-π EDA is an adsorption mechanism by bio-waste and the organic compounds. For example, the strong non-covalent p-electron donor-acceptor (EDA) interaction occurs between the graphene, which is similar to the bio-waste surface, and planar aromatic compound adsorption. The bio-waste surface can distribute charges of aromatic rings at a high temperature >1100 °C, but rough charge distribution at the temperature >500 °C. Moreover, the charge distribution of bio-waste with aromatic rings can increase or reduce its electron density, creating π-electron-rich or deficient systems (33). Aromatic-π systems in low-treatment temperature bio-wastes <500 °C containing electron-withdrawing entities may serve as electron-acceptors. Whereas, poly-condensed aromatic rings or electron-rich graphene sheets in high-treatment temperature bio-wastes could serve as π-donors that bind electron withdrawing molecules. The sorption affinity of atrazine to bio-waste was attributed to π-π EDA

interactions between the electron-withdrawing chlorine substituent in atrazine and the aromatic carbon on the surface of bio-waste (26). Also, at low pH, $\pi^+ \pi^-$ EDA interaction between the protonated aniline ring in sulfamethoxazole (SMX) and π-electron rich graphene surface of bio-waste was implicated in the sorption of SMX on giant-reed bio-waste. Furthermore, the adsorption of carbofuran by rice husk-derived bio-waste showed the π electron-rich bio-waste functional groups can be bonded with a protonated amino group of the carbofuran molecule forming strong π-π EDA interactions (34) (Figure 10).

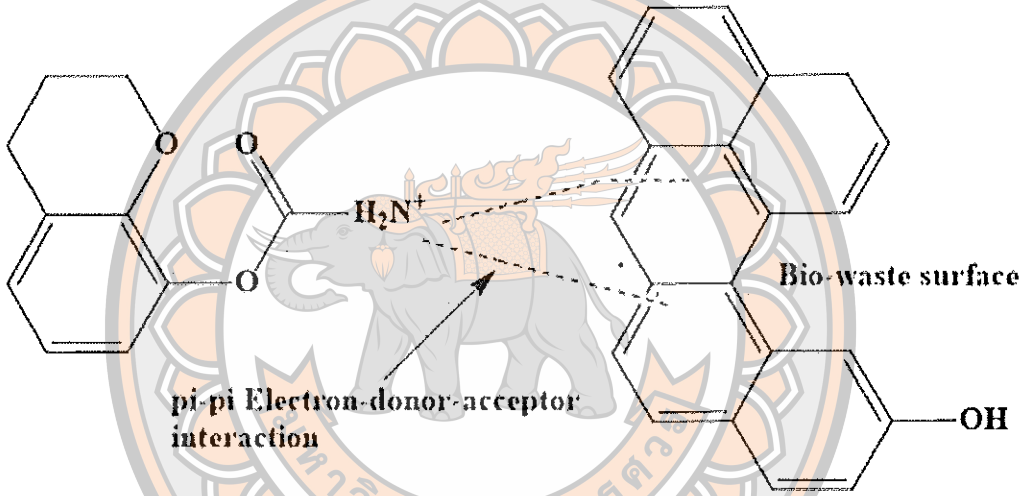

Figure 10 π-π EDA

Note: Adapted from S. S. Mayakaduwa et al. (34)

5. Cation-π interaction

Bio-waste including wastewater solids, animal-derived bio-wastes which have high Fe, Mg, Si, K or Ca as the cation-π can interact with the polycyclic aromatic hydrocarbons (PAH) of bio-waste (20). However, the hydrophobic or dispersive forces may be required to support such bonding.

6. Electrostatic interaction

Electrostatic interactions are the mechanism between ionic of pollutant and cationic of adsorbent, or vice versa. For example, if the organic compound is a cationic compound, which carried the positive charges will attract the negative charge of the adsorbents. In contrast, if the bio-waste is a cationic adsorbent, which carried the positive charge, will attach with the ionic absorbate (23). Moreover, pH can affect the adsorption process of bio-waste and adsorbates, because the surface of the bio-waste was controlled by the pH of the solution. If the solution pH is lower than the pH of point zero charges (pHpzc) of the bio-waste, then the surface of the bio-waste will be positively charged. If the solution pH is higher than the pHpzc of the bio-waste, the surface of the bio-waste will be negatively charged (20).

Additionally, when the electrostatic interaction between bio-waste and ionic, organic adsorbates are repulsive, increasing the ionic strength of adsorbate solutions will increase adsorption. But, increasing the ionic strength of adsorbate solutions when the electrostatic interaction is attractive, will reduce adsorption of the adsorbate. The adsorption of methylene blue (MB) decreased from 4.5 to 3 $mg.g^{-1}$ on CNT-modified bagasse bio-waste as ionic strength increased from 0.01 to 0.1 M NaCl, is likely due to competition between the Na^+ and MB^+ for negatively charged bio-waste sites (35).

According to (34) the electrostatic interaction between protonated carbofuran molecules and the negatively charged bio-waste surface may enhance the carbofuran adsorption.

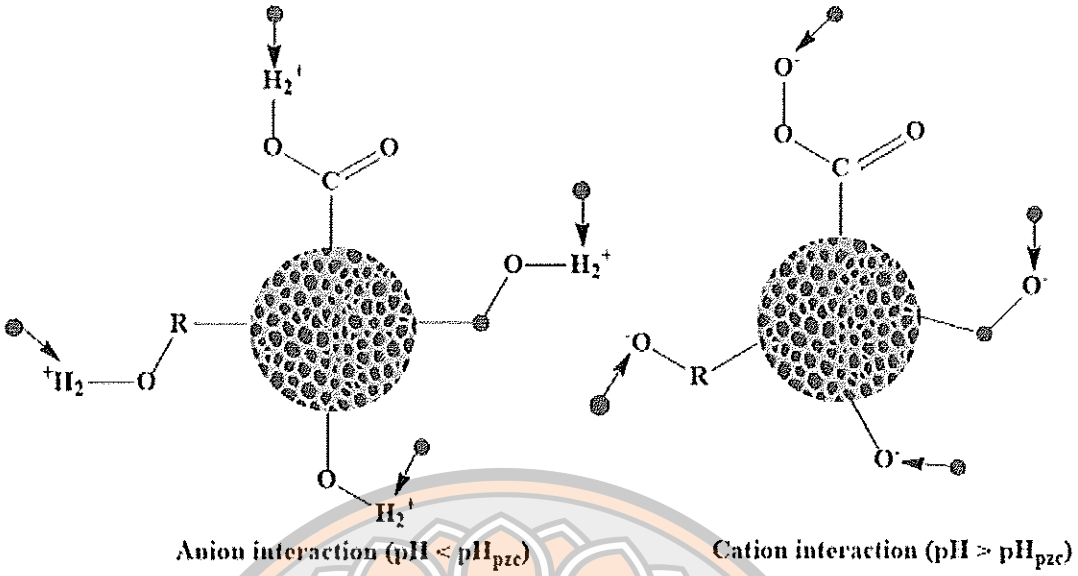

Figure 11 Electrostatic interaction

7. Diffusion and partitioning

There are many approaches of diffusion between pollutant and bio-waste such as diffusion of adsorbates into pores during pore filling interaction, or into the organic matter (OM) matrix of bio-waste non-carbonized fractions. According to (36), indicated that the organic pollutant has a tendency to partitioning into the non-carbonized organic matter and adsorption onto the carbonized matter. At the high solute concentration or in bio-waste which contain high volatile matter, the partition mechanism can occur in the last process. This condition can enhance the adsorption capacity due to the absorbed organic compound solute within the OM matrix. The partitioning on bio-waste can occur at the temperature ≤ 400 °C, which holds the small aromatic and aliphatic compounds such as pyrroles, phenols, ketones, and sugar. The porous nature of bio-waste can be the obstacle of organic pollutants diffusion. However, it does not have the difficulty in absorption of organic pollutants which contain hydrophobic molecules (20).

Adsorption isotherm

The process which explains the ions of molecules of a phase that has a trend to reduce the concentration on the surface of another phase was called adsorption. Adsorption is also the progress by which solid phase molecules stick to molecules of a gas or a liquid (37). The adsorbate is the fluid molecule attached to the surface of the adsorbent. Most of the adsorbents are the porous solid (38). The adsorption isotherm is vital in enhancing the adsorbents utilizing due to it describing how adsorbates interact with adsorbents (24).

1. Type of adsorption

Adsorption is used in all the natural systems including physical, biological, and chemical. It is also used in industries, for example, the activated carbon, bio-waste, synthetic resins. This method is appropriate for wastewater treatment as it is a simple and affordable process (39). The adsorption is controlled by two forces: physical forces called physical adsorption (physisorption) and chemical forces, i.e. chemical adsorption (chemisorption) (37).

1.1 Physical adsorption

The forces operation of physical adsorption is not strong. The molecules which adsorbed by the adsorbents are not stable on the surface of the adsorbents, they may move from one place to another. The power of energy which is used in physical adsorption is not more than 80 $kJ.mole^{-1}$. However, physical adsorption is easy to reverse (40).

1.2 Chemical adsorption

The forces of chemical adsorption are stronger that than a physical force due to the energy used in the adsorption of C-N bonds is 600 $kJ.mole^{-1}$. The chemical bonding is strong and hard to reverse. This is because of the chemical bond on the surface of adsorbate and the adsorbent are sharing of electrons. Sometimes on the same surface, both physisorption and chemisorption can occur at the same time, but the layer of the molecules is adsorbed by physisorption is on the upper and the chemisorbed layer is below (40).

2. Langmuir and Freundlich adsorption isotherm

The relationship between pollutants loading on the adsorbent and concentration of pollutants at equilibrium is determined using the Langmuir and the Freundlich isotherm models (22). A number of empirical models have been employed to analyse experimental data and define the equilibrium of pollutant adsorption onto the bio-wastes. The results are usually relevant to the properties of the bio-waste and the target pollutants. The parameters Q_0 and K_L of the Langmuir isotherm and the parameters K_f and n of the Freundlich isotherm were determined from the adsorption equilibrium data from the various samples (41).

2.1 Langmuir adsorption isotherm

The Langmuir isotherm model is used to assume the quantitatively of the monolayer adsorption without interaction between the adsorbed molecules. The Langmuir isotherm shows the accuracy of the monolayer adsorption on the surface of the adsorbent (41). The model assumes equal energy of the adsorption onto the surface. The Langmuir adsorption isotherm is shown below.

$$q_e = \frac{Q_0 K_L C_e}{1 + K_L Q_e} \quad (1)$$

The linear form of the Langmuir adsorption isotherm is presented below

$$\frac{1}{q_e} = \frac{1}{Q_0} + \frac{1}{Q_0 K_L C_e} \quad (2)$$

Where:

C_e (mg.L^{-1}) is the equilibrium concentration of pesticides

q_e (mg.g^{-1}) is the amount of the pesticide as adsorbed per gram of the bio-waste at equilibrium

Q_0 (mg.g^{-1}) is the maximum monolayer coverage capacity

K_L (L.mg^{-1}) is the Langmuir isotherm constant

From the slope and interception of the Langmuir isotherm plot of $1/q_e$ versus $1/C_e$, the Q_0 and K_L are calculated (41).

2.2 Freundlich adsorption isotherm

The Freundlich isotherm model is used to demonstrate the chemisorption process on the heterogeneous adsorption on the surface of the bio-wastes. The Freundlich equation is expressed below.

$$q_e = K_f C_e^{1/n} \quad (3)$$

Where:

K_f (mg.g^{-1}) (mg.L^{-1})$^{-n}$ is a Freundlich isotherm constant

n is the intensity of adsorption

The linear form of the Freundlich adsorption isotherm is as below:

$$\log q_e = \log K_f + \frac{1}{n} \log C_e \quad (4)$$

From the slope and intercept of the Freundlich isotherm plot of the *log* q_e versus *log* C_e, K_f and n were calculated (41).

Adsorption kinetic

Adsorption kinetics are used to study the relationship between the physical and/or chemical characteristics of the bio-wastes and display the strength of the relationship. The result of the adsorption kinetics can cause effects to the adsorption mechanism including mass transport and chemical reaction processes. The two most popular kinetic models used to study pollutant elimination by bio-wastes are the pseudo-first-order kinetic model and the pseudo-second-order kinetic model. These kinetic models provide valuable information which controlled the adsorption processes involving adsorbent surface chemical reactions.

1. Kinetic study

1.1 Kinetic study of pseudo-first-order and pseudo–second-order models

The amount of the bio-waste adsorption at time *t* and at equilibrium was evaluated by the equations below:

$$q_t = \frac{V(C_0 - C_t)}{W} \quad (5)$$

$$q_e = \frac{V(C_0 - C_e)}{W} \quad (6)$$

Where:

q_t & q_e (mg.g^{-1}) were the amounts of the bio-waste that is adsorbed at time *t* and at equilibrium

V (L) is the volume of pesticide solution

C_0, C_t, C_e (mg.L^{-1}) are the pesticide concentrations in the solutions at $t = 0$, $t = t$, and t = equilibrium, respectively

W (g) is the amount of bio-waste that was used (42, 43).

Two kinetic models including the pseudo-first–order (Eq.7) and pseudo–second–order (Eq.8) were applied to analyze the adsorption kinetics of pesticides and bio-waste. Both kinetic models described the kinetics of a solid–solution system, the pseudo-first-order showed mononuclear adsorption, whereas the pseudo-second-order illustrated binuclear adsorption (43). The equations are displayed below:

$$Log(q_e - q_t) = \log q_e - \frac{k_1 t}{2.303} \quad (7)$$

$$\frac{t}{q_t} = \frac{1}{K_2 q_e^2} + \frac{1}{q_e} t \quad (8)$$

Where: k_1 (h^{-1}) and k_2 (g.mg^{-1}.h^{-1}) are the adsorption rate constants of the pseudo-first-order and the pseudo-second-order models.

Effects of adsorption

The factors which can cause the effect of the adsorption efficiency by bio-waste consist of the properties of bio-waste, bio-waste residence time, pH, competitive anions, dosage of the adsorbent, temperature, bio-waste application rate, and pollutants species.

CHAPTER III

RESEARCH METHODOLOGY

Bio-wastes preparation

The three types of bio-waste including coconut fibre bio-waste (CF-BW), corn cob bio-waste (CC-BW), and bagasse bio-waste (BG-BW) were collected in Northern Thailand. Corn cob and bagasse are wet materials, thus they were left in the sun for a few days to extract the water before the synthesis process.

Bio-wastes were sliced into the approximate size (cm^{-1}) of 1 x 1 and dried in the oven at 105 °C for a few hours until getting the constant weight (Figure 12). The bio-wastes were burned in a furnace (Nabertherm, Germany) with the temperature slowly increased by 3 °C per minute. The pyrolysis process was conducted under oxygen-limited conditions at 600 °C for 4 hours as shown in Figure 13.

Corn cob Coconut fibre Bagasse

Figure 12 Bio-waste materials

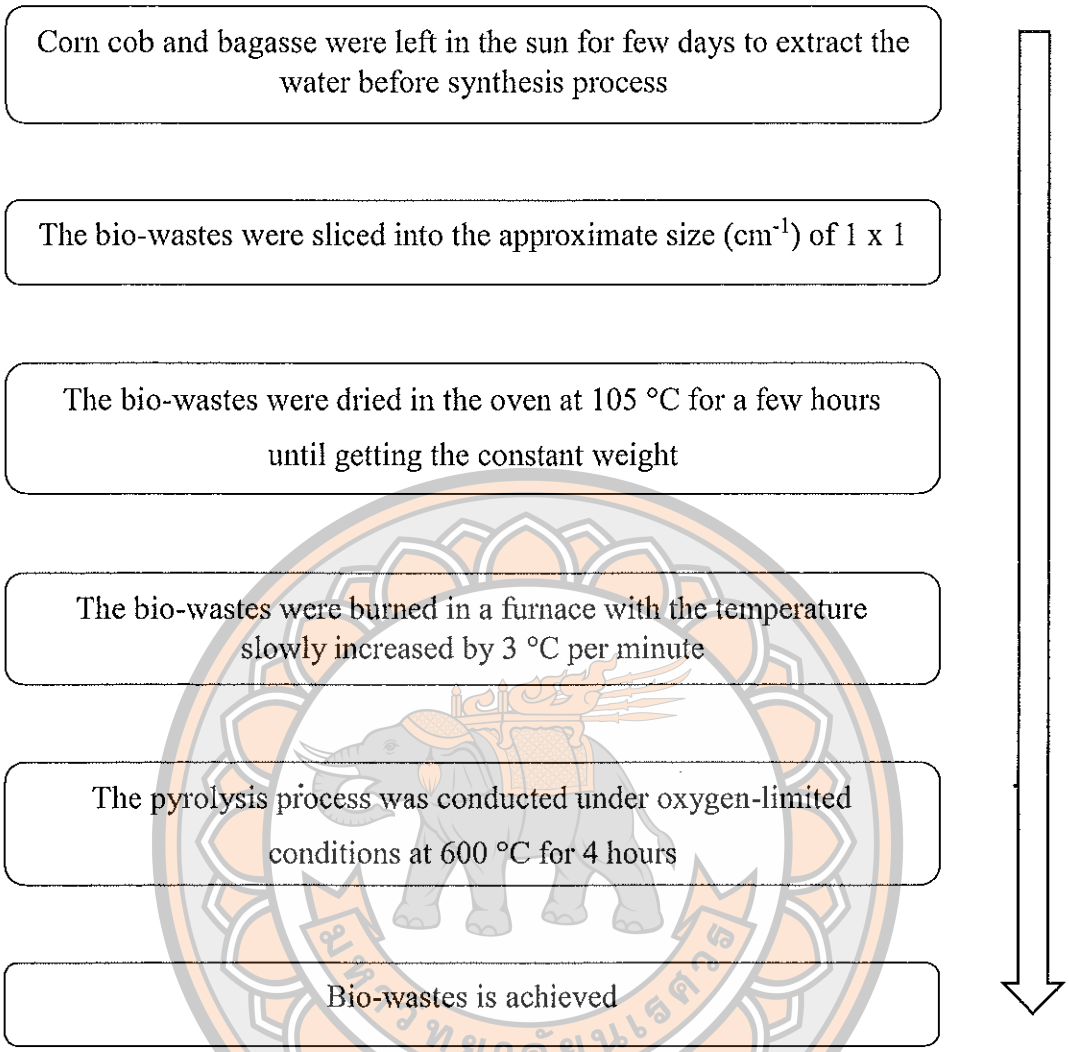

Figure 13 Bio-waste synthesized diagram

Bio-wastes modified by HF acid

After pyrolysis, bio-wastes were ground by pestle and mortar. Then sieved through a 0.8 mm mesh. To remove excess ash, the bio-wastes were washed with 0.1 M HF acid by following the method of the Minori Uchimiya group (44). After that, bio-wastes were washed with the deionized water until achieving the neutral pH. Finally, bio-wastes were dried in the oven at 80 °C overnight. The appearance of the final bio-waste material was a mixture of ash and charcoal. The processes of HF modified on bio-waste are shown in Figure 14.

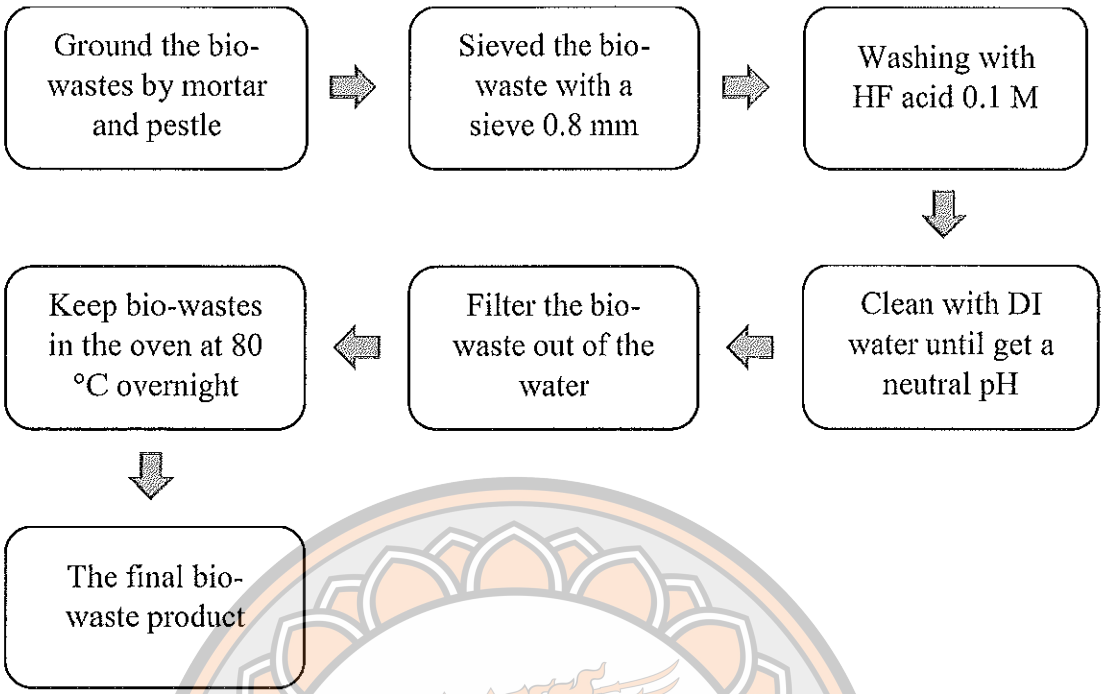

Figure 14 Processes of acid modification on bio-wastes

Bio-wastes characterization

The surface morphology and specific surface area of bio-wastes were analyzed by the Scanning Electron Microscope (SEM) model LEO 1455 VP (Carl Zeiss Microscopy GmbH, England) and the Brunauer–Emmett–Teller method (BET), respectively. The FT-IR (Frontier, PerkinElmer, Germany) method was applied to define the functional groups of the adsorbents.

Adsorption experiment

All the adsorption experiment will be performed by Erlenmeyer flask 250 ml and a shaker machine (MS Orbital Shaker, MS-NOR-30/MS-NOR-3001) in dark condition. Add the volume of pollutants into Erlenmeyer 250 ml and add an amount of bio-wastes into Erlenmeyer 250 ml. After that, the Erlenmeyer flask was placed on the shaker to perform the adsorption process. During the adsorption experiment, samples are taken to measure residual pollutants by UV–Vis spectrometer (Genesys 10S UV-Vis spectrophotometer, Thermo Scientific). A diagram of the adsorption experiment is shown in Figure 15 below.

The key parameter will study in the adsorption test:

1. Effect of pH to the adsorption experiment.

2. Effect of the initial concentration (7 concentrations) of pollutant to the adsorption experiment.

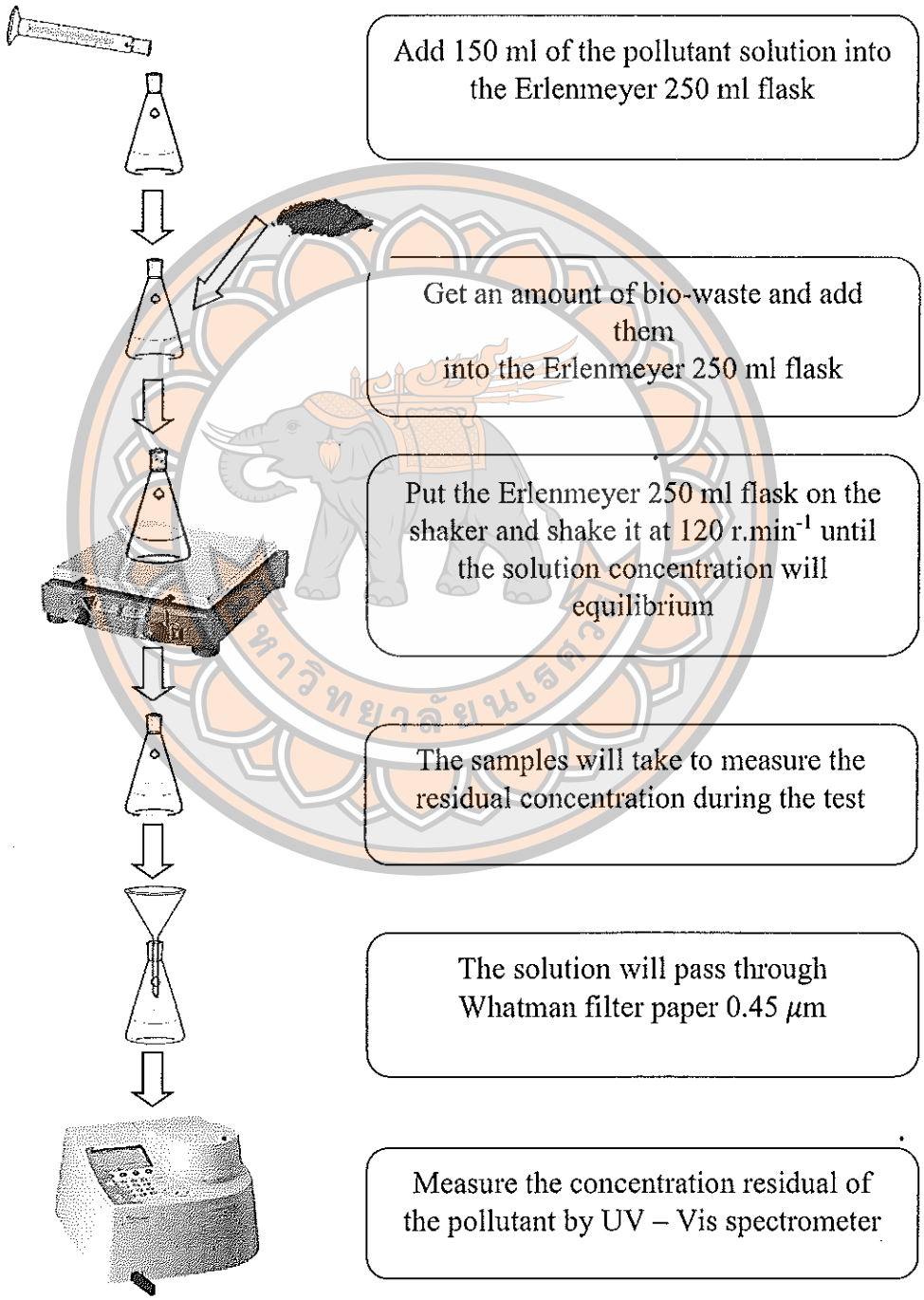

Figure 15 Flow diagram of the adsorption experiments of diazinon and bio-waste

1. Adsorption isotherm

There are two models of adsorption isotherm including the Langmuir isotherm model and Freundlich isotherm model. In this study, both models were investigated between three kinds of bio-waste consisting of corn cob, coconut fibre, and bagasse in diazinon removal. Adsorption isotherm results will show which bio-waste can be remove the pesticides with the greatest efficiency.

2. Adsorption kinetic

The adsorption kinetic models consist of the pseudo-first-order and pseudo-second-order model was discovered in this adsorption. Regarding the adsorption kinetic results, the best bio-waste mechanisms will appear in this study.

3. The adsorption mechanism of bio-wastes and diazinon

The adsorption mechanism of bio-waste and diazinon investigated in detail by using the theory of the adsorption mechanism of bio-waste and the evidence results. Furthermore, the infrared spectra of the bio-waste were recorded using the KBr press disk technique and a Fourier Transform-Infrared spectroscopy (FTIR, Perkin Elmer Spectrum, Germany), which recorded the 4000-400 cm^{-1} range at room temperature. The explanation of the mechanism results between bio-wastes and diazinon was supported by the FT-IR, SEM, and BET result.

Chemicals

Table 3 List of chemical used in this study

No	Name of chemical	Concentration (%)	Source
1	**HF**	48	Loba Chemie Pvt. Ltd, India
2	**H_2SO_4**	96	ACI Labscan, Thailand
3	**NaOH**	97	Ajax Finechem Pty. Ltd, Australia
4	**Diazinon**	60	SIMS AGROW CHEME CO., LTD, Thailand

Standard curve preparation

Pour 200 ml DI water into the 250 ml beaker. Add the diazinon according to the amounts stated in Table 4 to the water and stir with a glass rod until completely dissolved. Transfer the solution to a 1000 ml volumetric flask. Add DI water until the volumetric in the flask is 1000 ml (stock 1: primary standard).

Stock 2 of the diazinon in Table 4 were diluted from stock 1, to get 25 ml of stock 1 solution into a 50 ml volumetric flask and the volume was marked in 50 ml by DI water. Stock 1 and stock 2 were poured into brown glass bottles and kept in the refrigerator at 4 °C.

Preparing the working standard of the pesticide concentrations for the experiments are shown in Table 5. All these concentrations were diluted from stock 2 pesticide solutions and DI water and were performed in 150 ml volumetric flasks. The concentration of the diazinon calibration curve presented in Table 5.

Table 4 The standard calibration curve preparation of diazinon

Pesticide name	Diazinon
Amount of diazinon (60 w/v) in 1000 ml of solution	1.66 ml
Stock 1	1 000 $mg.L^{-1}$
Stock 2	100 $mg.L^{-1}$
The number of points	7

Table 5 The concentrations of diazinon for the calibration curve

The number of points	Working standard ($mg.L^{-1}$)	Stock 2 (ml) Concentration (100 $mg.L^{-1}$)	DI water (ml)
0	0	0	150
1	2.0	3	147
2	5.0	7.5	142.5
3	10	15	145
4	15	22.5	127.5
5	20	30	120
6	40	60	90
7	60	90	60

CHAPTER IV

RESULTS AND DISCUSSION

Characterization of bio-wastes SEM

1. Characterization of bio-wastes with non-acid-modified

The raw SEM of bio-wastes with non-acid-modified is shown in Figure 16. As the figures indicated that the pores of each bio-waste were blocked by minerals that the reason to make the pore size tiny. Moreover, it can reduce adsorption capacity. On the other hand, the amount of CF-BW' pores have more than other two bio-wastes pore.

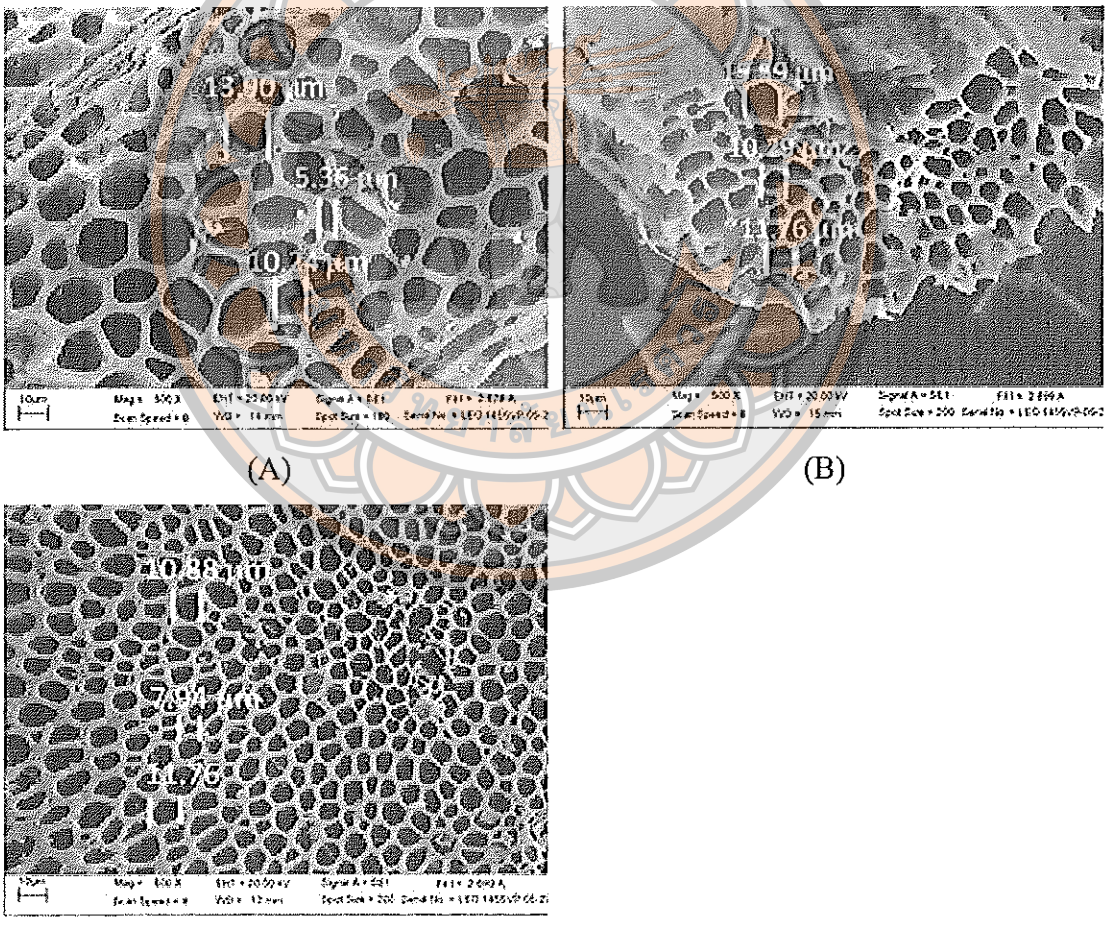

(A) (B)

(C)

Figure 16 SEM pictures of bio-wastes with non-acid-modified (A, B, C): CC-BW, BG-BW, CF-BW non-acid-modified, respectively

2. Characterization of bio-wastes after acid-modified

The surface morphology and pore size of the bio-wastes were changed after being acid-modified. The pores size of each bio-waste were clear with less or without blocked by the minerals as shown in Figure 17. As the results, it showed that acid treatment was the key factor to increase the specific surface area of bio-wastes which allowing higher adsorption capacities. Hence, the size of the surface morphology of the bio-wastes is the crucial element in the adsorption process.

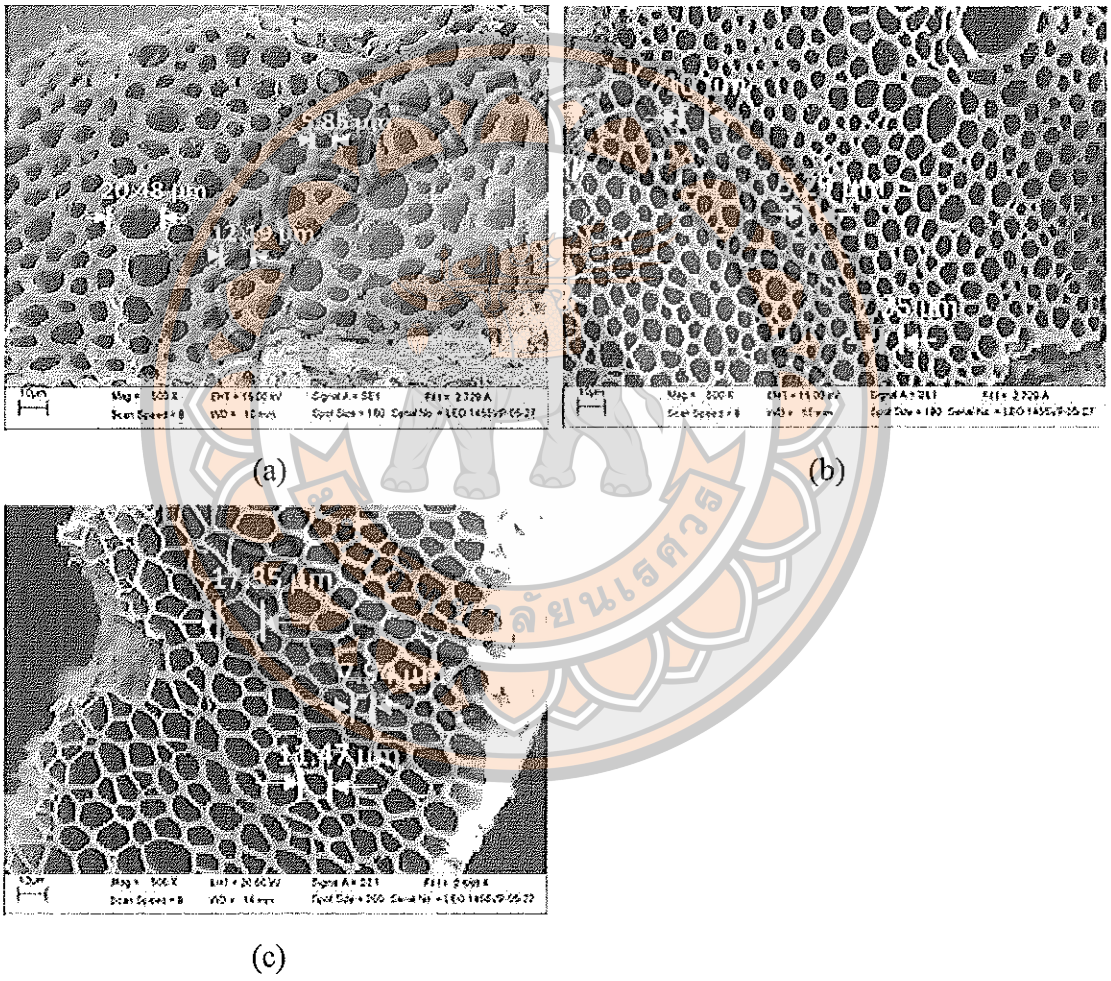

(a) (b)

(c)

Figure 17 SEM pictures of bio-wastes with acid-modified (a, b, c): CC-BW, BG-BW, CF-BW by HF modified, respectively

Specific surface area and total pore volume of bio-wastes

Three types of bio-waste were conducted by following the same condition to An Binh Quach method (45). Therefore, the value of specific surface area (BET), total pore volume (TPV), and pore volume dissemination was taking out by following his results. The results show that the specific surface area of CF-BW is higher than CC-BW and BG-BW in the ordering value 402.43 $m^2.g^{-1}$, 292.92 $m^2.g^{-1}$, and 67.42 $m^2.g^{-1}$, respectively. Noticeably, the BET is the main criteria to determine the adsorption capacity of bio-wastes. If the bio-waste has a large specific area on the surface, it has more interfaces for pollution adsorption (43). Likewise, the total pore volume of CF-BW (0.151 $cm^3.g^{-1}$) is also higher than CC-BW (0.117 $cm^3.g^{-1}$) and BG-BW (0.029 $cm^3.g^{-1}$). The result of pore distribution into four sizes including, micropores (<2 nm), narrow mesopores (2-20 nm), mesopores (21-50 nm), and macropores (>50 nm). The micropores (<2 nm) of CF-BW, CC-BW, and BG-BW were 17.40%, 21.24%, 16.88%, respectively. The narrow mesopores (2-20 nm) of CF-BW, CC-BW, and BG-BW were 69.22%, 56.57%, 59.29%, respectively. The mesopores (21-50 nm) of CF-BW, CC-BW, and BG-BW were 6.10%, 10.39%, 15.75%, respectively. The macropores (>50 nm) of CF-BW, CC-BW, and BG-BW were 7.28%, 11.81%, 8.07%, respectively. The majority of pore volumes of bio-wastes were narrow mesopores and micropores. Additionally, the specific surface area has a positive correlation with micropore volume because the pore size distribution is a key factor responsible for the increase in surface area in bio-waste (23).

The TPV is the main factor for the high adsorption of bio-wastes. The pore size of bio-wastes is very important in achieving the uptake of adsorbate (46). Noticeably, the pores size of bio-waste acted as a potential factor in the pore-filling mechanism.

FT-IR of the bio-wastes

The results of the surface functional groups of adsorbents were demonstrated by FT-IR analysis. The FT-IR spectras of the bio-waste are exhibited in Figure 18. There are eight main functional groups in a different spectrum which appeared on the surfaces of the bio-wastes. Moreover, among of the eight main functional groups, there is three main interaction including H-bonding, hydrophobic, and π-π EDA interaction that caused by those functional groups.

1. H-bonding functional groups

The band 3000-3600 cm^{-1} and peak at 3789 cm^{-1} were hydroxyl groups (O-H) stretching vibrations of carboxylic acid, alcohol, and phenol (47).

The bands at 1216 cm^{-1} and 1217 cm^{-1}, represented the aromatic C-O stretching of phenolic hydroxyl (48). The bands at 1045 cm^{-1}, 1070 cm^{-1}, and 1099 cm^{-1} of CC-BW, CF-BW, and CC-BW, respectively, were recognized to the aromatic C-O stretching of alcohol (49).

The peaks around 1736 cm-1, 1734 cm^{-1}, and 1715 cm^{-1} of bio-wastes were assigned to the carbonyl group C=O and could show ketone, carboxylic acid, and ester. These groups can cause H-bonding interaction (50). The bands at 2298-2383 cm^{-1} were ascribed to the ketone group C=O (51). Moreover, the hydroxyl groups (O-H) are presented with significant H-bonding interaction.

2. Hydrophobic functional groups

The results indicated that the functional groups which can cause hydrophobic interaction had two types such as aromatic C-H and Aliphatic group. Aromatic C-H bands were around 744-878 cm^{-1} and Aliphatic C-H bands were 2845-2915 cm^{-1}.

3. π-π EDA functional groups

There is one functional group that can be generated the π-π EDA interaction is aromatic C=C. The bands of aromatic C=C is shown about 1563-1571 cm^{-1} (49, 51).

In brief, all the functional groups were summary in Table 6. The major functional groups of the adsorbents including ketone, carbonyl, and aromatic organic molecules which are unsaturated hydrocarbons. The hydroxyl group is also the main molecule on the bio-wastes. All these functional groups can cause H-bonding interaction between bio-wastes and diazinon (50). Furthermore, the aromatic group of the bio-wastes has the π-π EDA interaction with the diazinon (50) when the alkyl group has hydrophobic properties (52).

Furthermore, the transmittance of CF-BW is lowest if compare to another two transmittances of CC-BW and BG-BW. This is showed that the surface of CF-BW has many functional groups more than another two bio-wastes.

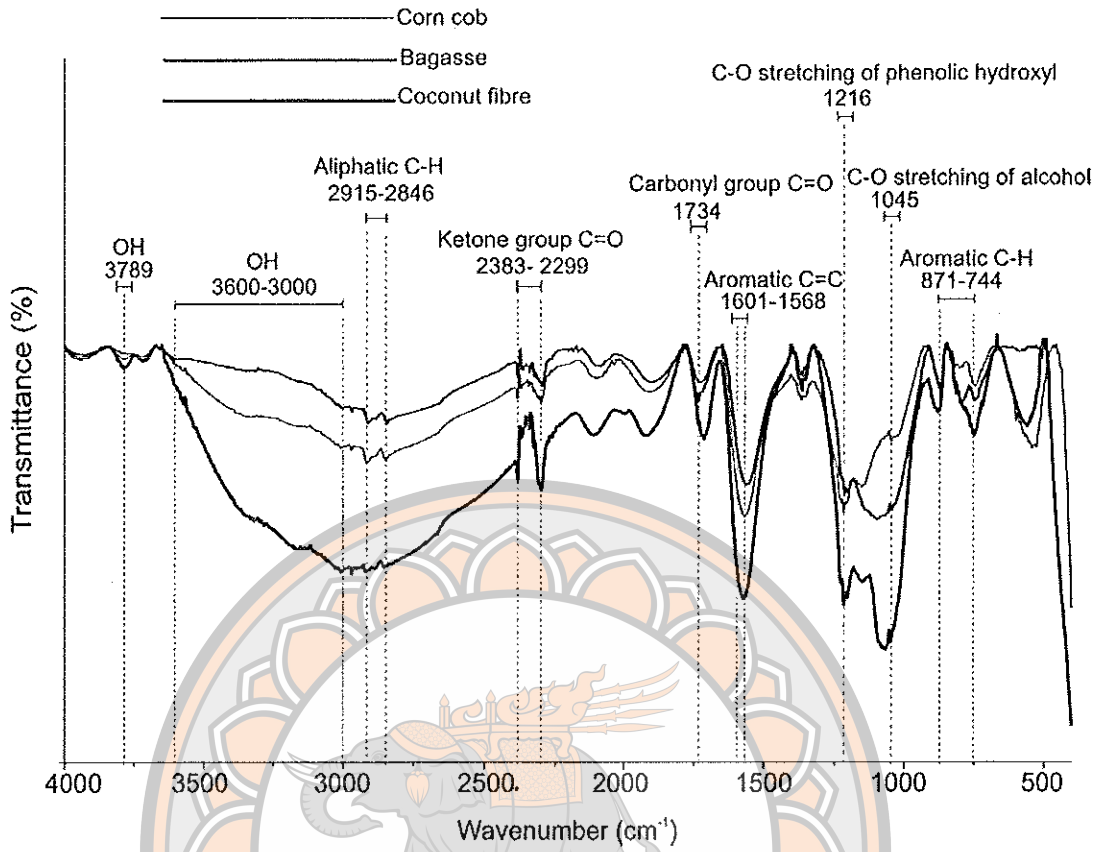

Figure 18 FT-IR spectrum analysis of bio-wastes

Table 6 FT-IR spectra results of the optimum bio-wastes

The functional groups of bio-wastes	CC-BW	BG-BW	CF-BW	Ref.
	Wavenumber (cm^{-1})			
Aromatic C-H	871-744	847-748	878-750	(47)
C-O stretching of alcohol	1045	1099	1070	(49)
C-O stretching of phenolic hydroxyl	1216	1216	1217	(48)
Aromatic C=C	1568	1563	1571	(49, 51)
Carbonyl group C=O	1734	1736	1715	(50)
Ketone group C=O	2383-2299	2382-2298	2354-2299	(51)
Aliphatic C-H	2915-2846	2911-2845	2915-2845	(52)
OH group	3600-3000	3600-3000	3600-3000	(47)

The adsorption mechanism of bio-wastes and diazinon

Chemical adsorption was generated by the interactions between the functional groups of bio-wastes and the diazinon. The proposed chemical interaction of diazinon and bio-wastes adsorption contain H-bonding, hydrophobic, and π-π EDA interactions regarding the results of FT-IR in Figure 20.

The pore-filling, hydrogen bonding, electrostatic, hydrophobic, and π-π EDA interactions were the adsorption mechanism between bio-wastes and diazinon (24) as shown in Figure 21.

1. Pore-filling

In this study, the SSA and the TPV results of bio-wastes before and after diazinon adsorption were different. This validated that the pore-filling mechanism and chemical interaction occurred between adsorbents and diazinon adsorption. According to the pore size data from section 4.2, the CC-BW, BG-BW, and CF-BW had a high distribution of micropores (<2 nm) and narrow mesopores (2-20 nm), in the range between 21.24 and 56.57 %, 16.88 and 59.29%, and 17.40 and 69.22%, respectively. The sorption of organic sorbates onto adsorbents by pore-filling mechanisms is a function of its total micropore and mesopore volumes (20). Furthermore, the dimension of the molecular structure of diazinon was 1.08 x 0.58 x 1.04 nm (0.65 nm^3) analysed by using the ChemBio3D software as shown in Figure 19. The data of the bio-wastes pore size were quite close to the structural size of diazinon. Hence, the diazinon can be adsorbed into micropores and narrow mesopores of the bio-wastes. Additionally, the pore-filling mechanism happened when the pore size of adsorbent is close to the molecular structure size of adsorbate (53).

The reduction of SSA and TPV determined the occupied diazinon in the pores of bio-wastes. This revealed that the pore-filling mechanism occurred between the bio-wastes and diazinon.

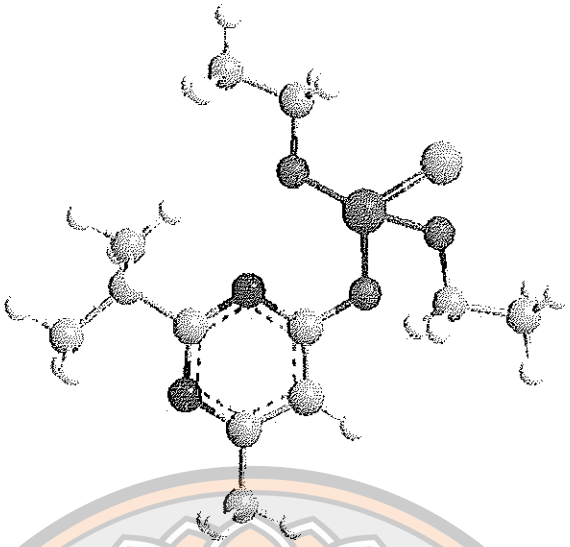

$(1.08 \times 0.58 \times 1.04\ nm) = 0.65\ nm^3$

Figure 19 Dimension of diazinon analysed by ChemBio3D software

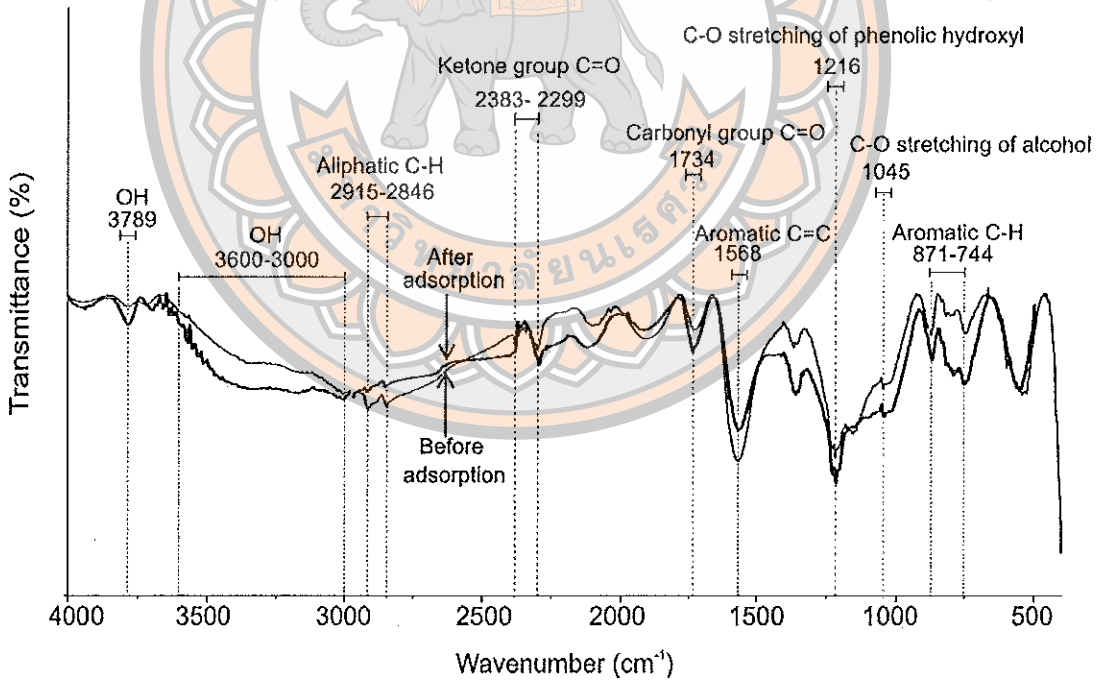

CC-BW

Figure 20 FT-IR analysis of bio-wastes before and after diazinon adsorption

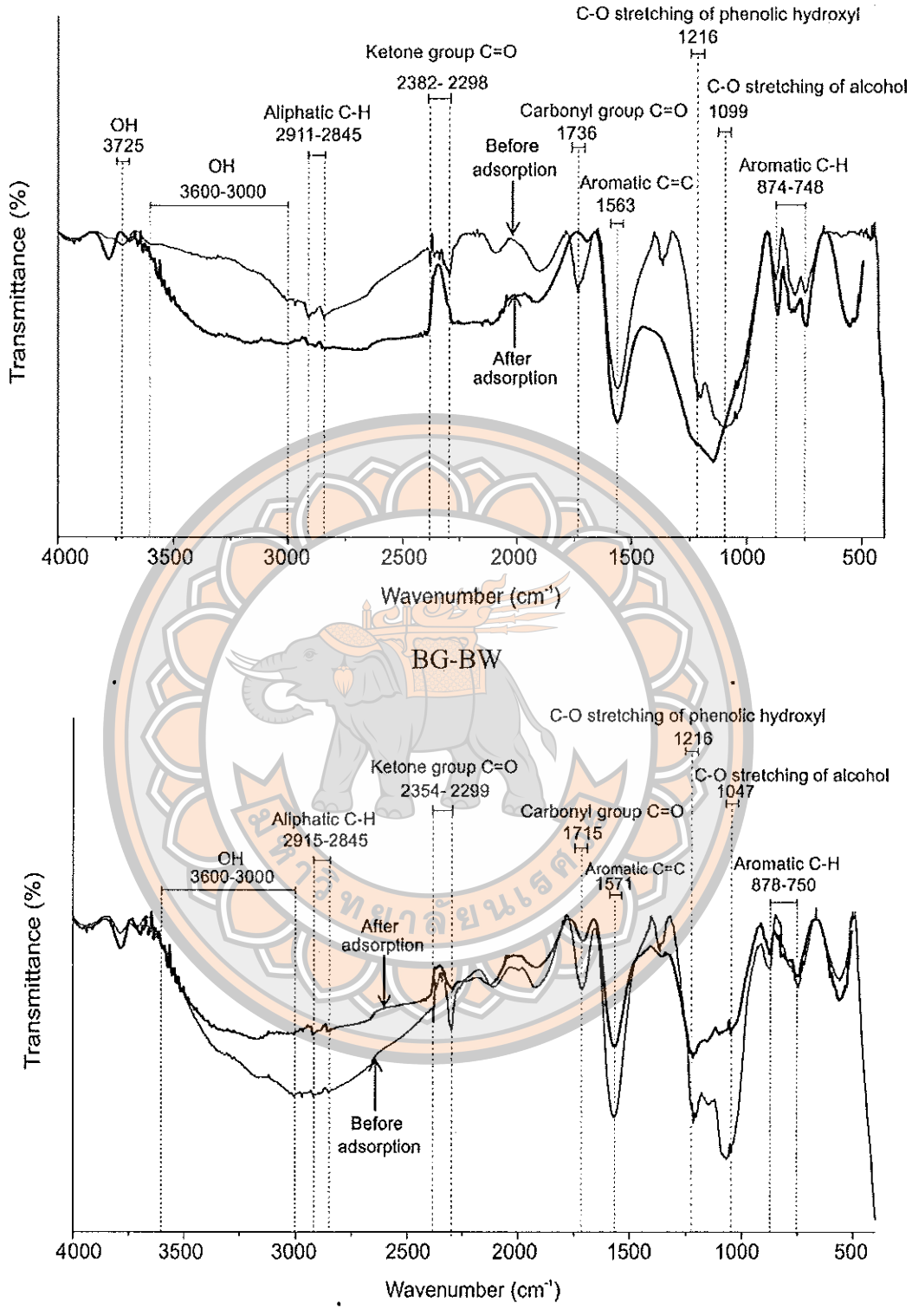

Figure 21 FT-IR analysis of bio-wastes before and after diazinon adsorption

Table 7 FT-IR of bio-wastes before and after diazinon adsorption

Wavenumber (cm^{-1})	Ascribed to the type of vibration	The functional group	Proposed interactions	Ref.
1045-1099	C-O	C-O stretching of alcohol	H-bonding	(54)
1216	C-O	C-O stretching of phenolic hydroxyl	H-bonding	(54)
1563-1571	C=C	Aromatic hydrocarbon	π-π EDA	(55)
1715-1736	C=O	Carbonyl group	H-bonding	(54)
2299-2383	C=O	Ketone group	H-bonding	(54)
2845-2915	C-H	Aliphatic C-H	Hydrophobic	(52)
3600-3000	O-H	Alcohol, phenol, carboxylic acid	H-bonding	(56)

2. H-bonding

Figure 20 displays the formation of H-bonding and the shift of FT-IR results after diazinon adsorption. The peak and peak area were assigned to the C-O stretching of alcohol (1045 cm^{-1}) and phenolic hydroxyl (1216 cm^{-1}), C=O of carbonyl group (1734 cm^{-1}), C=O of ketone group (2383-2299 cm^{-1}), O-H of alcohol, phenol, and carboxyl (3600-3000 cm^{-1}) which were changed as shown in Figure 20. All of the peaks suggest that O and H atoms in these functional groups were involved in H-bonding interactions (54). According to (56), carboxylic acid and the phenolic groups of bio-wastes could act as hydrogen donors. Therefore, an H atom from alcohol, phenol, and carboxyl groups of the diazinon engendered the H-bonding interaction with O atom from bio-wastes by harmonizing to the previous research (56). This type of interaction is shown in Figure 21.

At pH 4, the proton (H^+) was added to the N atom which caused the N atom has a negative charge due to protonation of N atom of the pyrimidine ring which generated more electrons. Moreover, the electronegativity of C atom was lower than N atom in the pyrimidine ring, this led to a positive charge on the nucleus and a negative

charge on the N atom. The N atom of the pyrimidine ring of diazinon can form an H-bonding interaction with H from the functional groups including hydroxyl and carboxylic of bio-waste as depicted in Figure 21.

In addition, the H atom from group of carboxylic acid and phenolic of bio-waste can cause H-bonding with the phosphate O linked to the pyrimidine ring in organophosphate pesticide which was a possible force for the sorption interaction (57). This interaction was agreed with Olivella et al. (2015), reported that the H-bonding between H from the adsorbent and the O atom in pollutant provided a significant contribution to the uptake of pollutant (58).

3. Hydrophobic interaction

The peak areas 2845-2911 cm^{-1}, which represented the alkyl group were changed after diazinon adsorption as shown in Figure 20. The intensity change of alkyl group of bio-wastes after diazinon adsorption was dissimilar. The aliphatic C-H group of CF-BW was shift greater than BG-BW, while the CC-BW graphs were not almost changed. However, the aromatic C-H of CC-BW was changed greater than BG-BW and CF-BW but in the insignificant percentage. This results showed that the CC-BW contained aromatic ring more than CF-BW and BG-BW. Likewise, the alkyl groups of bio-wastes also presented hydrophobic properties (52). Hence, the hydrophobic bond can be formed from alkyl side chains from diazinon, and alkyl groups (aliphatic and aromatic) from the bio-wastes by depicted in Figure 21.

4. π-π EDA interactions

The changing of the peaks showed that the aromatic C=C which was related to the π-π EDA interactions. The π-π EDA interactions of the bio-wastes after diazinon adsorption is shown in Figure 20. The π-π EDA interactions will be stronger when increasing the amount of hydroxyl due to, a hydroxyl group can act as an electron providing group (55). In this adsorption, there are many hydroxyl groups of bio-wastes which can be providing the electron, this leads to the aromatic rings of bio-wastes to be high in electron density (π^-). Moreover, in the pyrimidine ring where the N atom had more electronegativity than a C atom, caused the dipole in the pyrimidine ring to create a negative charge on the N atom and a positive charge on the nucleus ($\pi+$). So, π-π EDA interactions were formed between diazinon and the aromatic hydrocarbon compound of the bio-wastes. Besides, the intensity change of CF-BW on aromatic C=C functional

group was greater than BG-BW and CC-BW. This is indicated that the surface of CF-BW contained the aromatic C=C functional group more than another two bio-waste. Previous studies have shown that π-π EDA interactions are much stronger than Van der Waals forces (26). Therefore, the high adsorption affinity between the diazinon and the bio-wastes may have resulted from specific interactions between the diazinon molecules and the bio-waste surface.

In summary, several functional groups of bio-wastes including, alcohol, phenol, and carboxylic acid groups, showed the H-bonding interaction. The alkyl group of bio-waste presented the hydrophobic interaction and the aromatic group of bio-wastes presented the π-π EDA interaction. There are many functional groups can caused H-bonding. Moreover, the presence of polar groups such as O-alkyl groups and carboxyl carbons can decrease the accessibility of aromatic compounds of bio-wastes to pesticides (26, 50). This may be ascribed to strong H-bonding interactions occurred between polar groups on the bio-wastes and diazinon. Thus, H-bonding was the primary and major interaction that played an important role in chemical adsorption. Lastly, the adsorption mechanism between the bio-wastes and diazinon consisted of the pore-filling sorption mechanism and the chemical interaction including H-bonding interaction, hydrophobic interaction, and π-π EDA interaction as depicted in Figure 20 and 21.

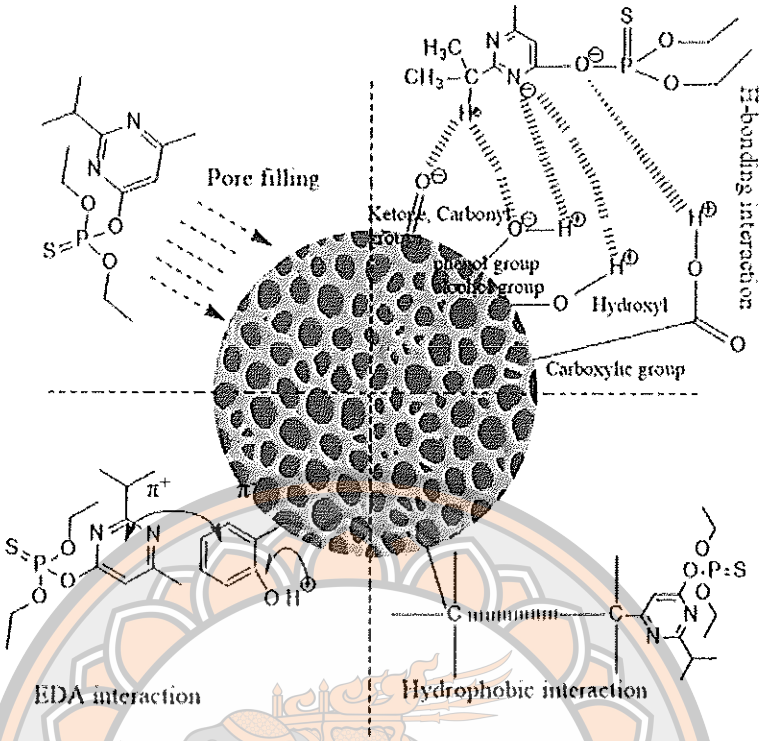

Figure 22 A depiction of adsorption mechanism between bio-wastes and diazinon

Effect of the pH on diazinon adsorption

pH is one of the factors affecting the quality of groundwater and surface water. 95% of groundwater, pH is in the range of 5.5-9 and in 80% of the water, it is in the range of 6.5-8.5. Moreover, pH is the main factor that affects adsorption efficiency between adsorbent and adsorbate (11). Hydrolysis of diazinon in aqueous solutions depends on the temperature of the aqueous environments so that the pesticide has small thermal stability and is rapidly degraded by increasing the environmental temperature (59). It should be noted that the effect of diazinon hydrolysis has been considered in the calculated removal percentage. The hydrolysis percentage of diazinon at various pH levels was determined with experiments in a condition similar to those of adsorption tests except no adsorbent was added to the solution (11). A greater degree of hydrolysis was observed in pH levels that were acidic (60). Therefore, in this study, the temperature during all adsorption processes was considered 24±2 °C. Moreover, diazinon hydrolysis is accelerated in an acidic solution (61).

In this study, the value pH from 2 to 10 was investigated. The pH of solution influenced the diazinon removal was indicated in Figure 22. From the result, it can be observed that the efficiency of diazinon removal increased when pH values increased to pH 4 but decreased gradually when the pH values are higher than pH 4. However, the electrostatic interaction was engendered by the surface of bio-wastes and diazinon, depending on pH changes in the solution. The percentage of the highest removal of diazinon was succeeded at the pH 4.0, which was not performed by the electrostatic attraction. As a reason, at pH 4, the diazinon was formed as negatively charged due to the pH of the solution was higher than the pKa (2.6). Whereas, the surface charges of the bio-wastes were negatively charged when the pH of the solution was adjusted higher than the pHpzc (0.7) value (45). Hence, the electrostatic of diazinon adsorption by bio-waste is repulsion reaction. Nevertheless, according to Teixidó et al. (2011) reported that the electrostatic repulsion between negatively charged anionic organic compounds and bio-wastes could promote H-bonding and induce adsorption (62). Additionally, another research found that the protonation of hydroxyl group on the adsorbent and protonation of nitrogen atoms on the diazinon pyrimidine groups in acidic pH can cause increasing the diazinon removal efficiency (63). In brief, the electrostatic attraction is not the primary mechanism for the anionic adsorption of diazinon onto bio-wastes, which deviates from the traditional understanding of anion binding. However, the hydrogen bonding, hydrophobic, pore-filling, and π-π EDA interactions can act as factors in this adsorption.

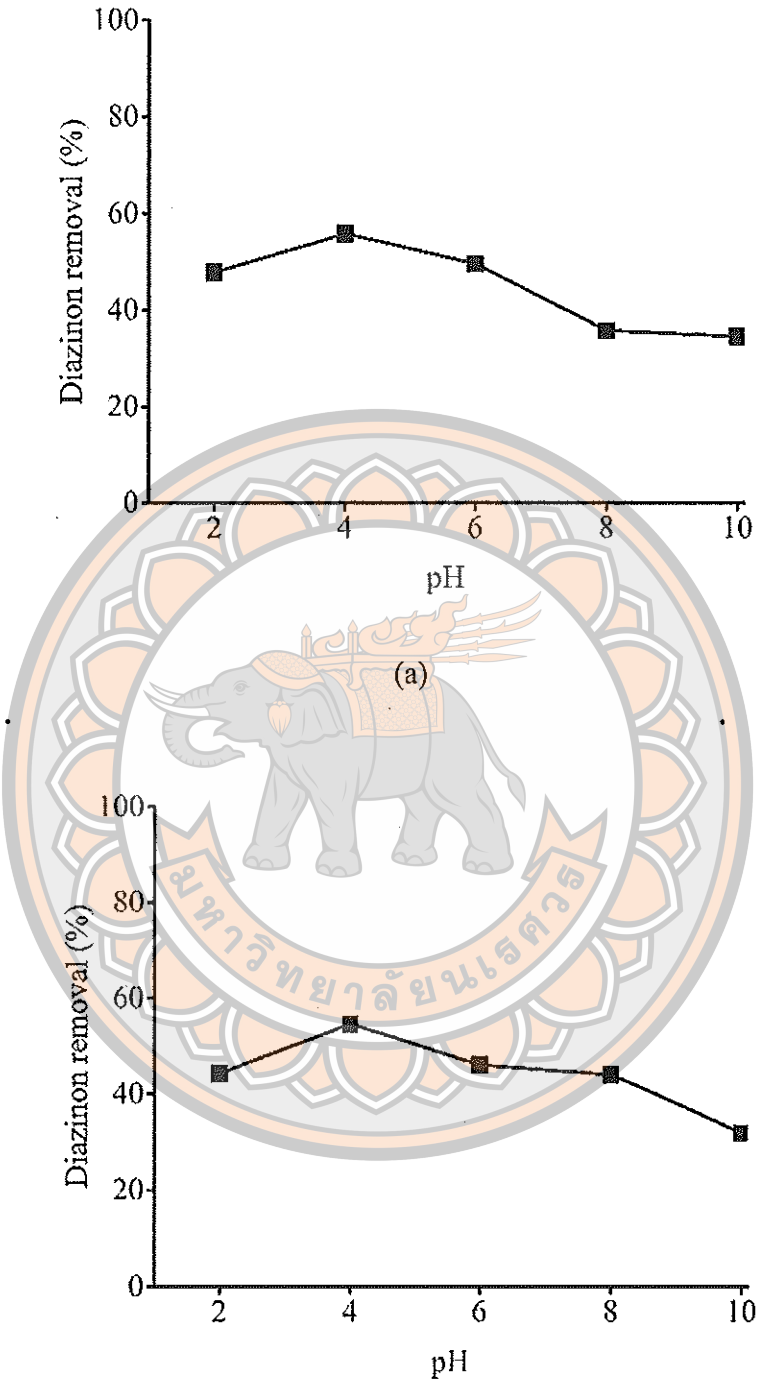

Figure 23 The influence of pH on the efficiency of diazinon removal by bio-wastes (a) CC-BW, (b) BG-BW, and (c) CF-BW

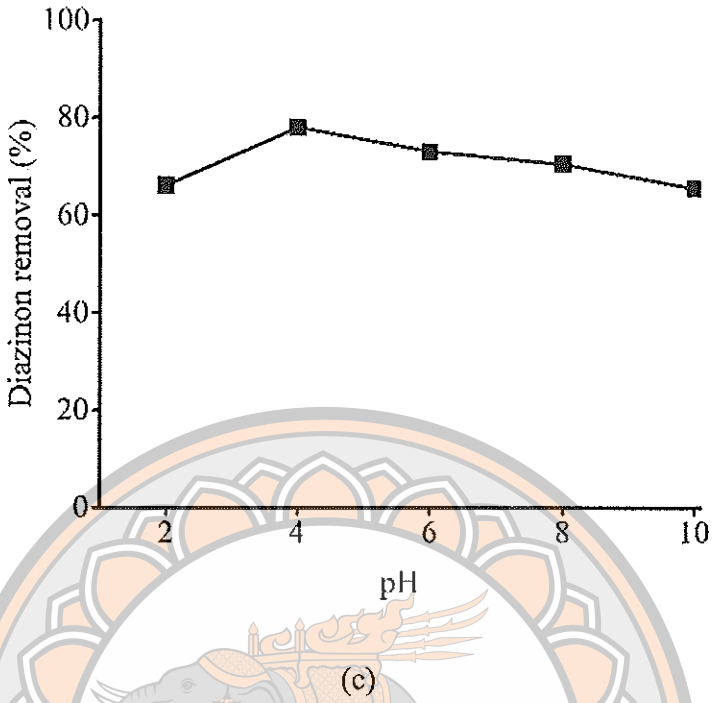

Figure 24 The influence of pH on the efficiency of diazinon removal by bio-wastes (a) CC-BW, (b) BG-BW, and (c) CF-BW

The isotherm adsorption models

The adsorption isotherms including Langmuir and Freundlich models of diazinon and bio-wastes are shown in Figure 23 and Table 8. The results showed that the Langmuir model of bio-waste adsorption was more appropriate than the Freundlich model due to the corresponding correlation coefficient R^2 of the Langmuir model were higher than the R^2 Freundlich model. These factors demonstrated that the monolayer adsorption of diazinon occurred on the surface of bio-wastes. Regarding R_L values in the adsorptions were lower than 1, illustrated the form of the isotherm is favourable for adsorption

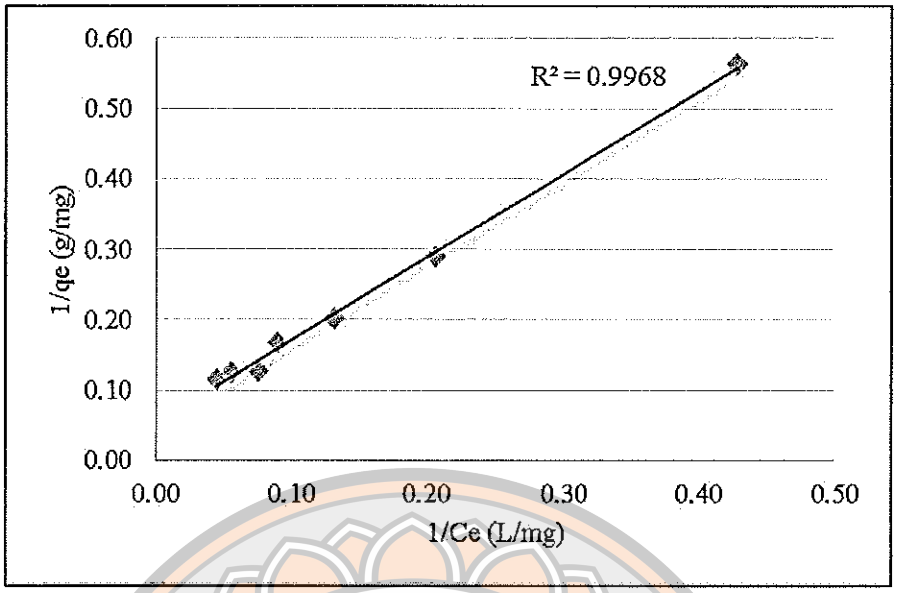

(A)

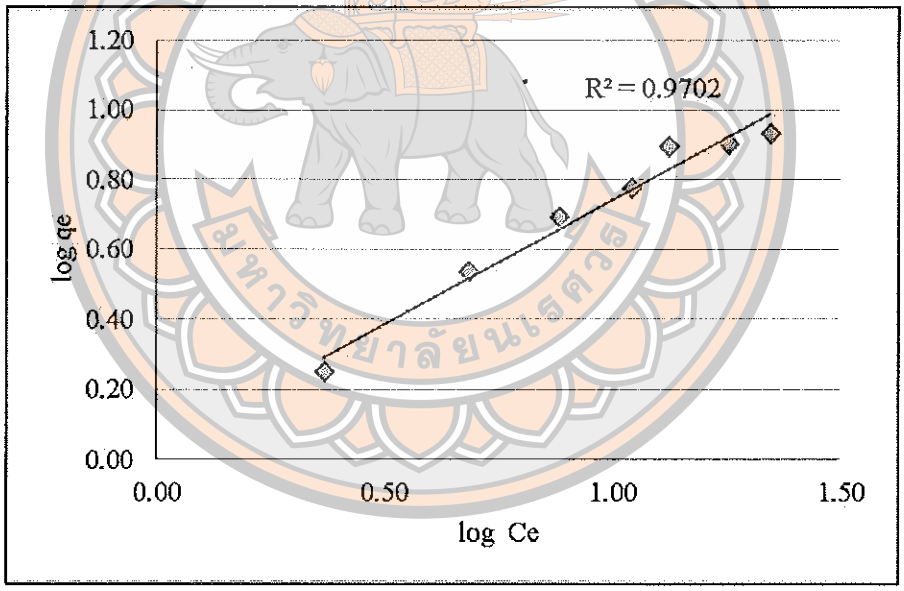

(a)

Figure 25 Adsorption isotherms of diazinon adsorption onto bio-wastes: (A) CC-BW-Langmuir model, (a) CC-BW-Freundlich model (B) BG-BW-Langmuir model, (b) BG-BW-Freundlich model (C) CF-BW-Langmuir model, (c) CF-BW-Freundlich model

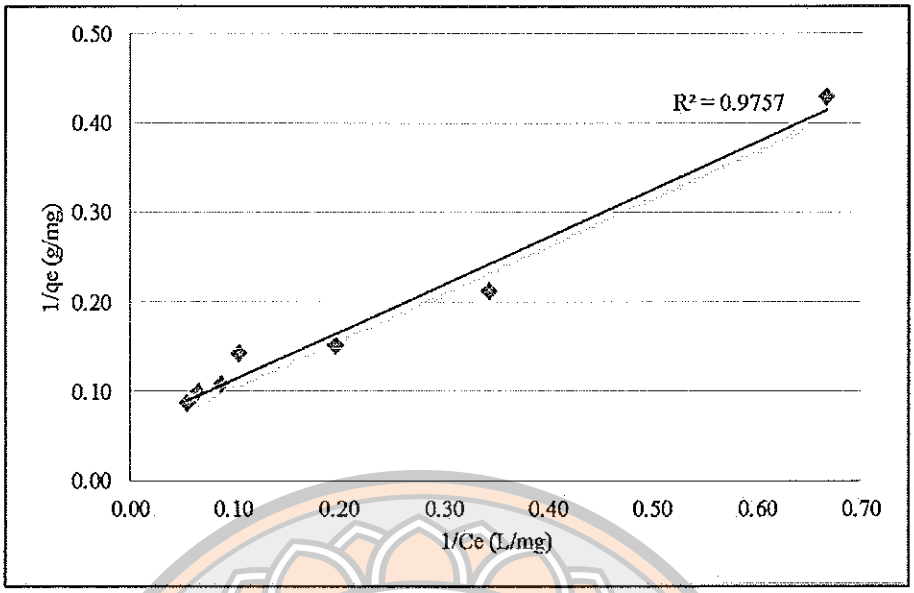

(B)

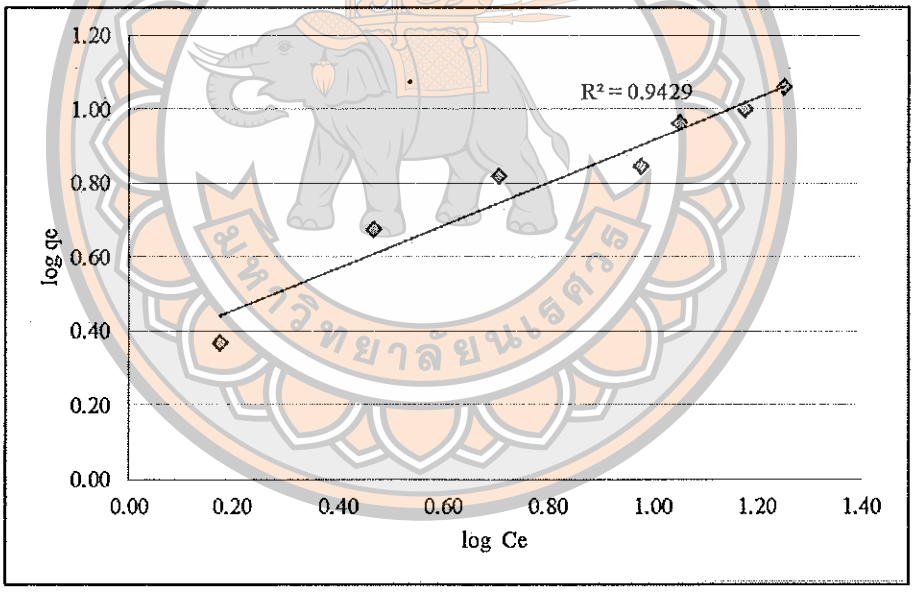

(b)

Figure 26 Adsorption isotherms of diazinon adsorption onto bio-wastes:
(A) CC-BW-Langmuir model, (a) CC-BW-Freundlich model
(B) BG-BW-Langmuir model, (b) BG-BW-Freundlich model
(C) CF-BW-Langmuir model, (c) CF-BW-Freundlich model

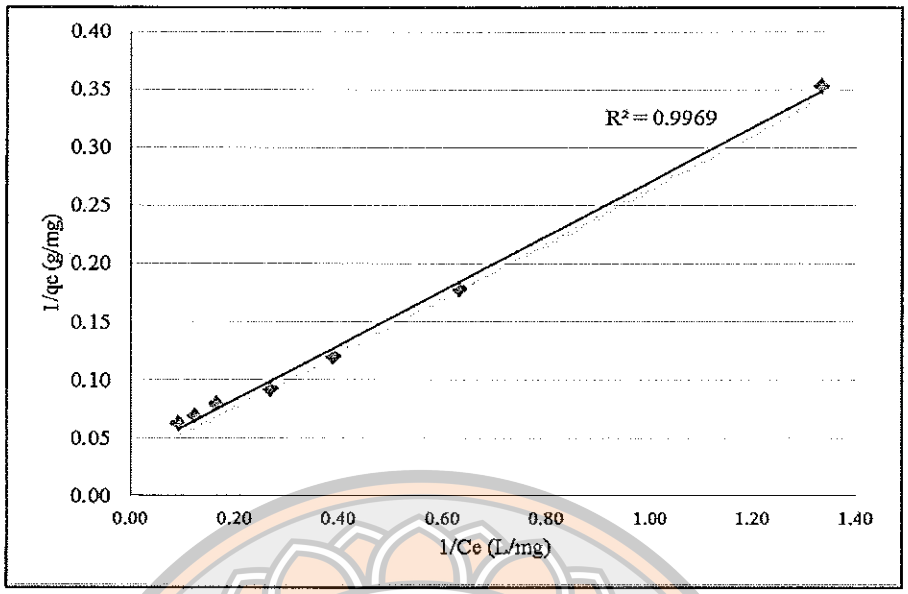

(C)

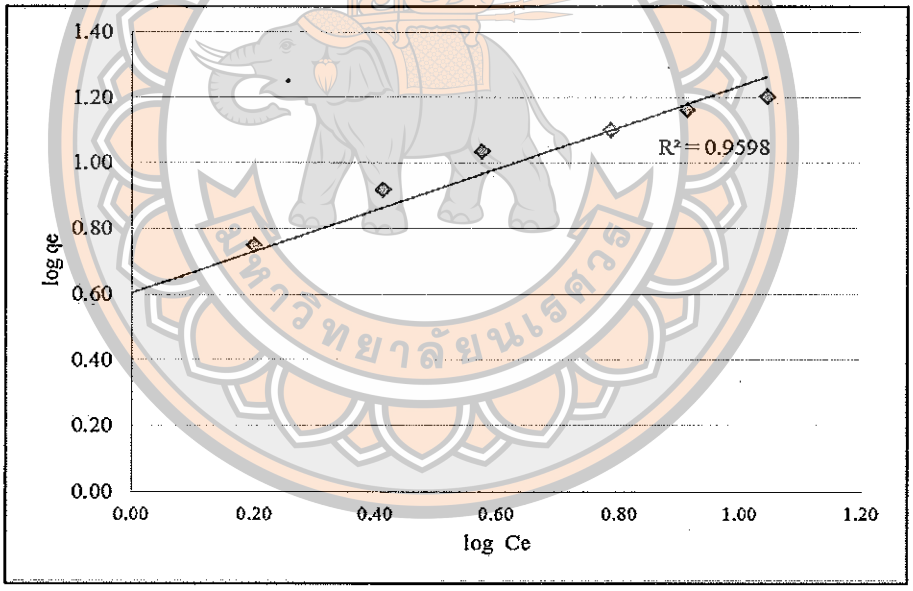

(c)

Figure 27 Adsorption isotherms of diazinon adsorption onto bio-wastes:
(A) CC-BW-Langmuir model, (a) CC-BW-Freundlich model
(B) BG-BW-Langmuir model, (b) BG-BW-Freundlich model
(C) CF-BW-Langmuir model, (c) CF-BW-Freundlich model

Table 8 The isotherm of the adsorptions

Models	Parameters	Bio-wastes		
		CC-BW	BG-BW	CF-BW
Langmuir	Q_0 ($mg.g^{-1}$)	18.80	16.50	27.60
	K_L ($L.mg^{-1}$)	0.050	0.110	0.160
	R_L	0.467	0.269	0.205
	R^2	0.996	0.975	0.997
Freundlich	K_F ($mg.g^{-1}$) $(mg.L^{-1})^{-n}$	1.071	2.178	4.000
	1/n	0.702	0.642	0.641
	R^2	0.970	0.942	0.959

The kinetic adsorption models

Study of adsorption kinetics is one of the important parameters because it provides good information about the mechanism of the adsorption process (64). Besides, adsorption kinetics displays a strong relationship with the physical and/or chemical characteristics of the bio-waste. The result of adsorption kinetics influences the adsorption mechanism, which may involve mass transport and chemical reaction processes (24).

Most of the studies used the pseudo-first-order and pseudo-second-order kinetic models to study the adsorption of water pollutants onto bio-wastes. However, to clarify the adsorption kinetic between diazinon and bio-wastes, the first-order model (FO) and second-order model (SO) were calculated from the experiment data and plot the graph as shown in Figure 24. In addition, the pseudo-first-order model (PFO) and pseudo-second-order model (PSO) were utilized to determine the experimental results in this study. Parameters from fittings included the sorption capacity (q_e), rate constants (k_1 and k_2) and respective R^2 values, are shown in Table 9 and Figure 25. The result showed that the q_e values calculated from the PFO were significantly divergent to the q_e value of the experimental data whereas the q_e values calculated from the PSO were confirmed as fitting to the q_e the experimental data. The PSO' graphs of each bio-waste adsorption are straight lines if compare to graphs of PFO. Furthermore, the R^2 values of

bio-wastes were closed to 1 and higher than the R^2 values of the PFO. As observed q_e values, plots of data R^2 values between PSO and PFO, confirming that adsorption of diazinon onto bio-wastes can be described by the PSO model than the PFO.

The adsorption had the best fit to the PSO model, exhibited that the adsorption predominantly describes the chemisorption process and the functional groups on adsorbents had interaction with the pollutant (35, 64). The functional groups of bio-wastes consisted of phenol, alcohol, ketone, carbonyl, and aromatic hydrocarbons, which caused interactions between diazinon and bio-wastes as clarified in the above section. The chemisorption for the PSO model consists of the exchange of electrons, covalent forces, and ion exchange (65). However, the chemisorption of diazinon and bio-wastes was the H-bonding, hydrophobic, and π-π EDA interactions.

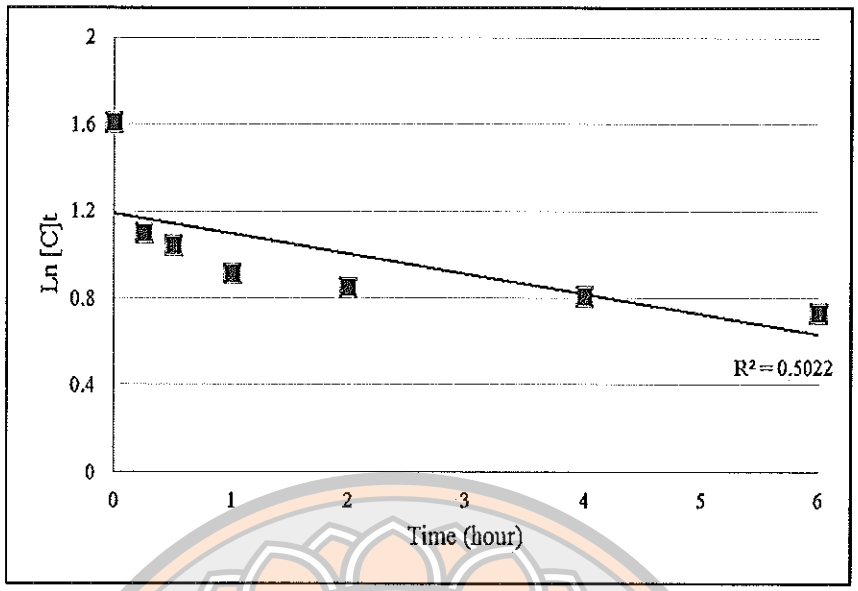

(A)

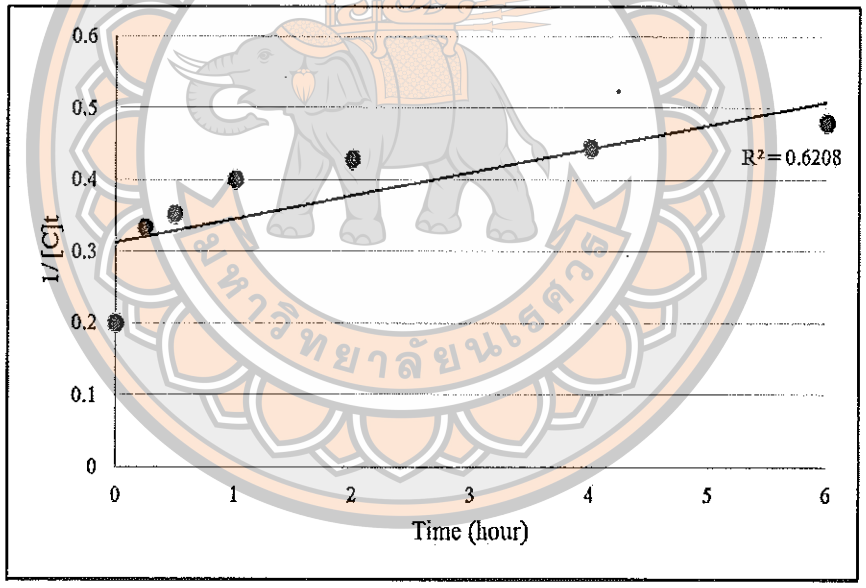

(a)

Figure 28 Adsorption kinetics of diazinon adsorption onto bio-wastes:
(A) CC-BW-FO model, (a) CC-BW-SO model
(B) BG-BW-FO model, (b) BG-BW-SO model
(C) CF-BW-FO model, (c) CF-BW-SO model

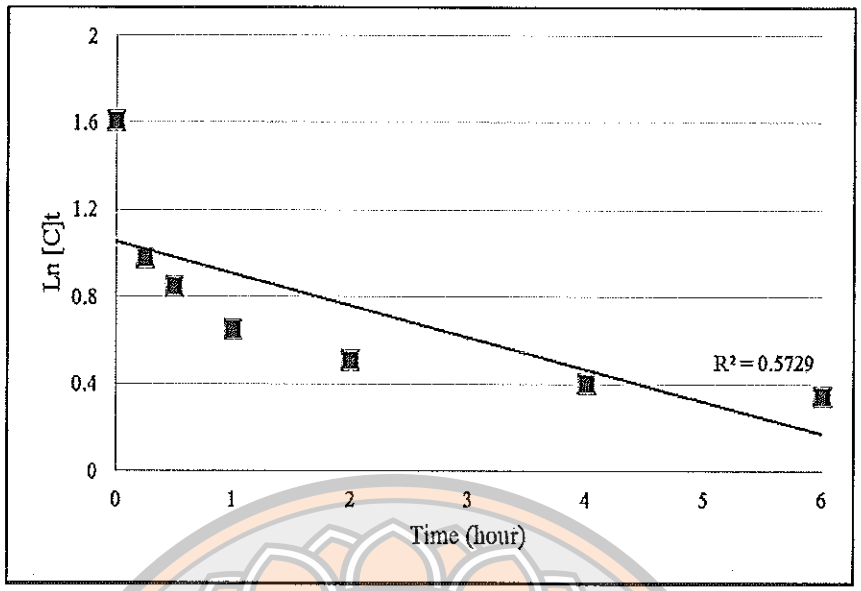

(B)

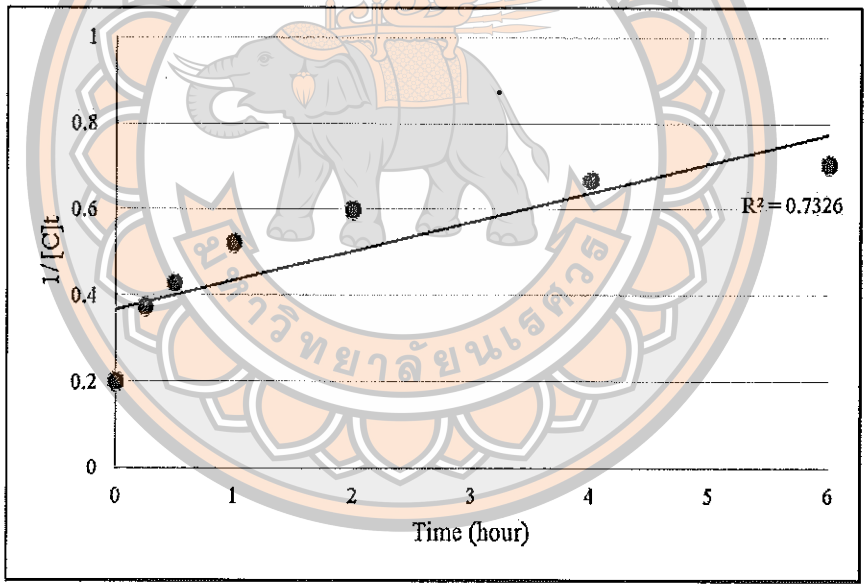

(b)

Figure 29 Adsorption kinetics of diazinon adsorption onto bio-wastes:
(A) CC-BW-FO model, (a) CC-BW-SO model
(B) BG-BW-FO model, (b) BG-BW-SO model
(C) CF-BW-FO model, (c) CF-BW-SO model

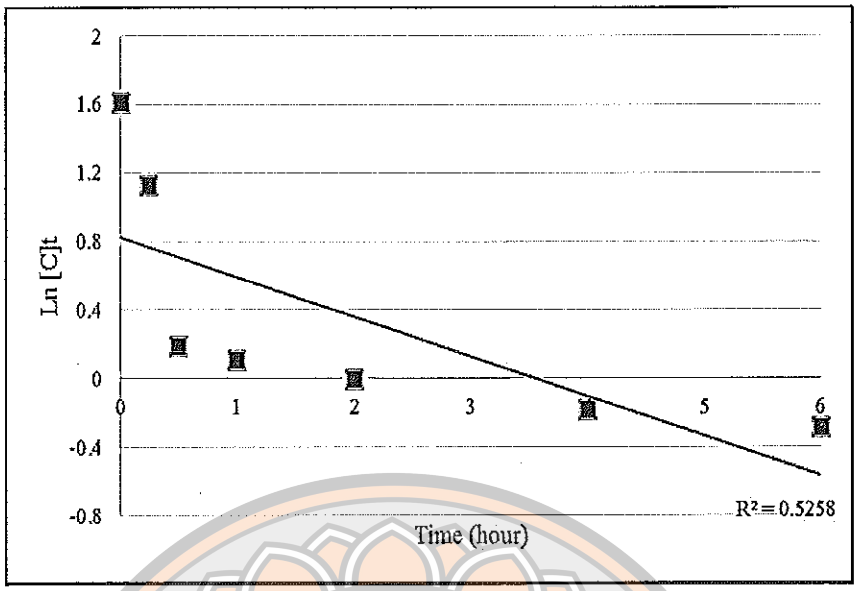

(C)

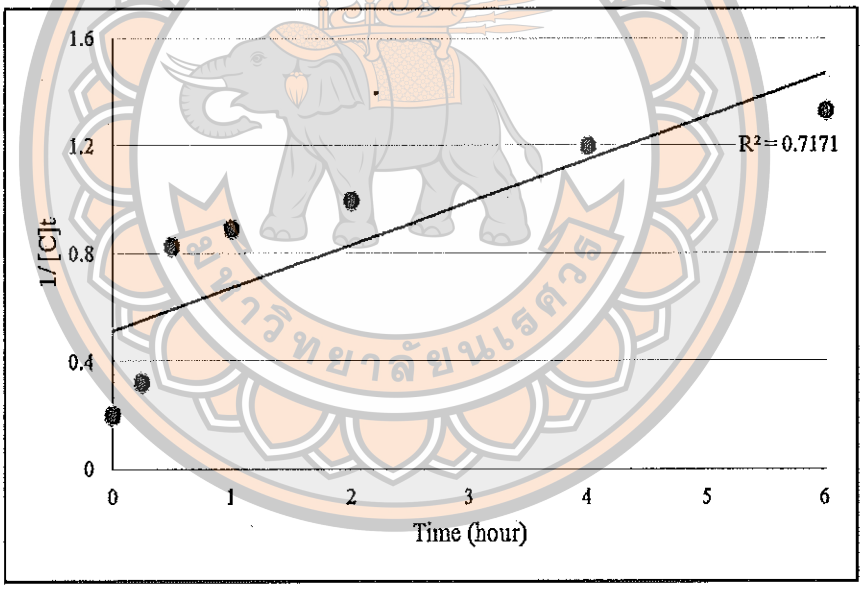

(c)

Figure 30 Adsorption kinetics of diazinon adsorption onto bio-wastes:
(A) CC-BW-FO model, (a) CC-BW-SO model
(B) BG-BW-FO model, (b) BG-BW-SO model
(C) CF-BW-FO model, (c) CF-BW-SO model

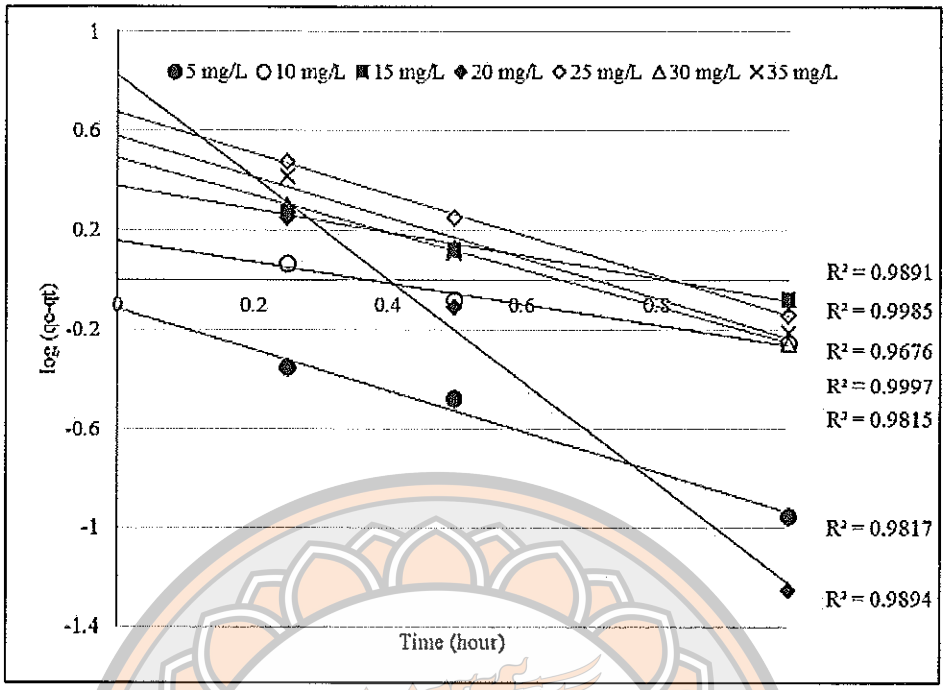

(A)

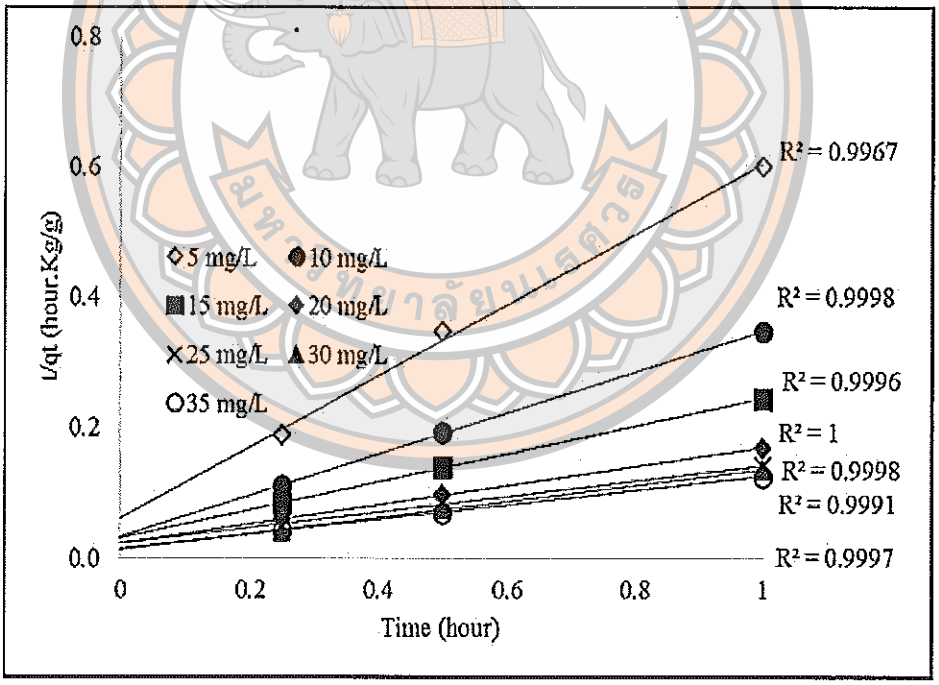

(a)

Figure 31 Adsorption kinetics of diazinon adsorption onto bio-wastes:
(A) CC-BW-PFO model, (a) CC-BW-PSO model
(B) BG-BW-PFO model, (b) BG-BW-PSO model
(C) CF-BW-PFO model, (c) CF-BW-PSO model

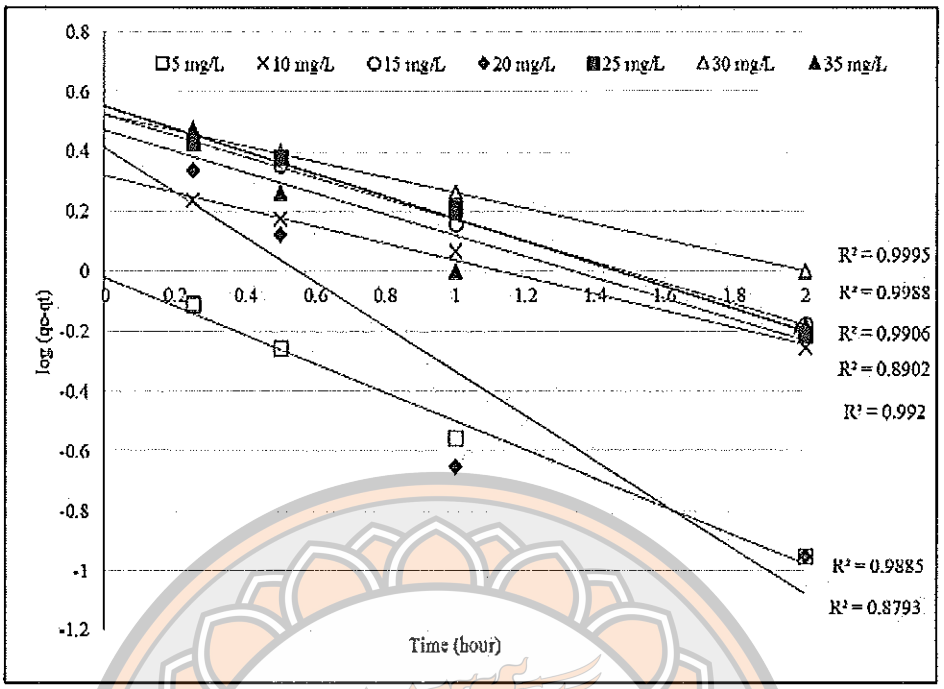

(B)

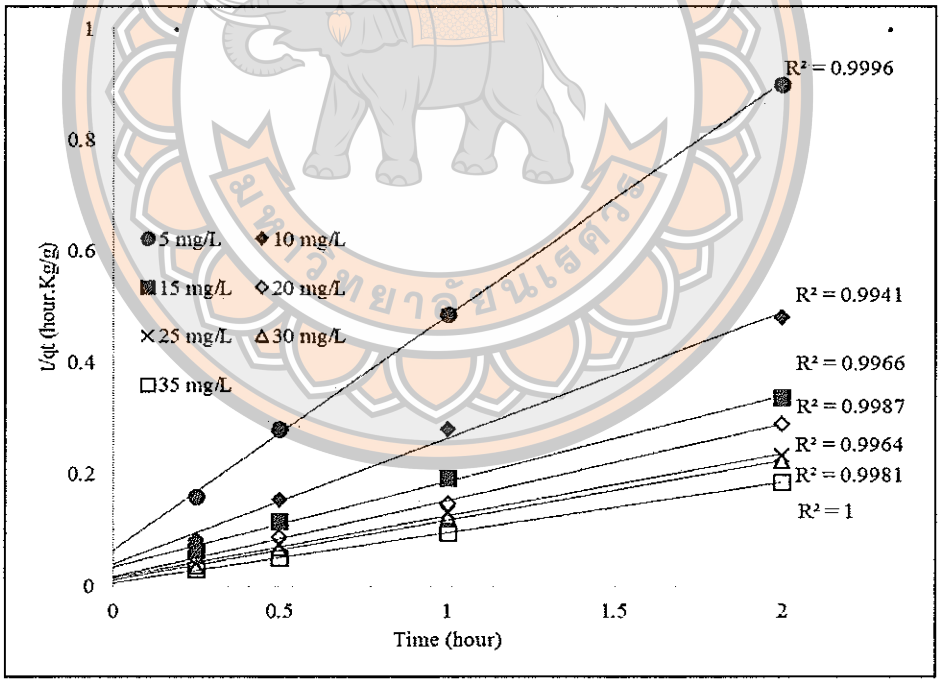

(b)

Figure 32 Adsorption kinetics of diazinon adsorption onto bio-wastes:

(A) CC-BW-PFO model, (a) CC-BW-PSO model

(B) BG-BW-PFO model, (b) BG-BW-PSO model

(C) CF-BW-PFO model, (c) CF-BW-PSO model

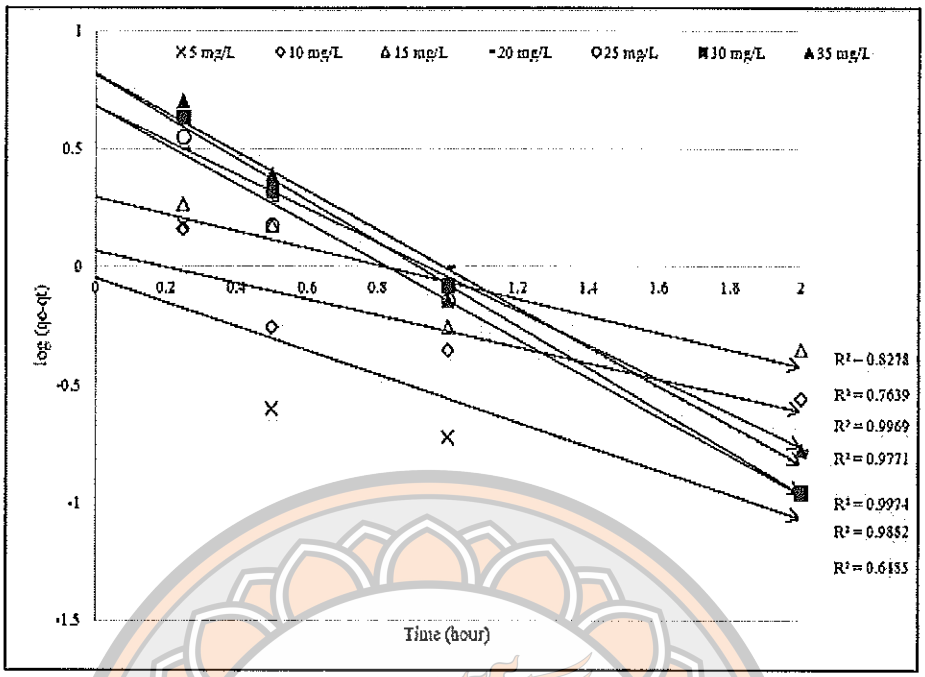

(C)

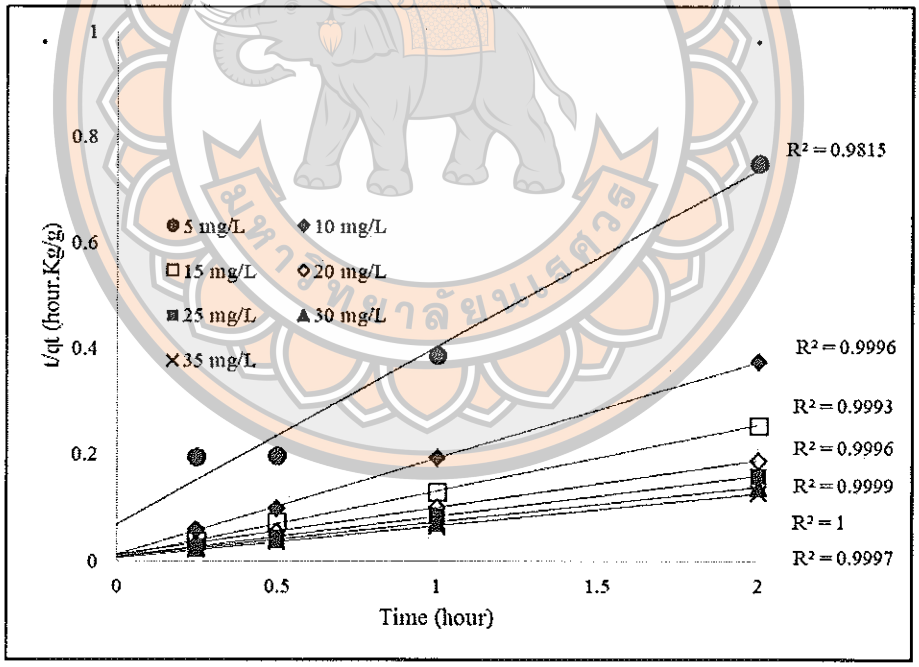

(c)

Figure 33 Adsorption kinetics of diazinon adsorption onto bio-wastes:

(A) CC-BW-PFO model, (a) CC-BW-PSO model

(B) BG-BW-PFO model, (b) BG-BW-PSO model

(C) CF-BW-PFO model, (c) CF-BW-PSO model

Table 9 Kinetic parameters for diazinon adsorption onto bio-wastes

BWs	Initial con. ($mg.L^{-1}$)	q_e exp ($mg.g^{-1}$)	PFO parameters		PSO parameters	
			q_e, calc. ($mg.g^{-1}$)	k_1 (h^{-1})	q_e, calc. ($mg.g^{-1}$)	k_2 ($g.mg^{-1}h^{-1}$)
CC-BW	5	1.78	0.77	1.849	1.98	2.70
	10	3.44	1.43	0.989	3.83	1.05
	15	4.94	2.39	1.091	5.14	1.03
	20	6.00	6.66	4.622	9.55	0.81
	25	7.83	4.71	1.899	8.17	0.82
	30	7.99	3.10	1.708	8.29	1.14
	35	8.60	3.78	1.937	8.95	1.01
BG-BW	5	2.33	0.96	1.112	2.45	2.23
	10	4.72	2.09	0.647	4.90	0.70
	15	6.61	3.34	0.804	6.88	0.50
	20	7.00	2.59	1.698	7.26	1.23
	25	9.16	3.55	0.842	9.27	0.61
	30	9.99	3.34	0.595	10.35	0.44
	35	11.44	2.95	0.860	11.74	0.68
CF-BW	5	2.83	0.90	1.488	2.99	1.78
	10	5.61	1.17	0.942	5.52	2.95
	15	8.28	1.98	0.810	6.73	1.48
	20	10.83	4.79	1.683	10.79	1.08
	25	12.61	4.78	1.981	13.13	0.75
	30	14.55	6.50	2.086	12.26	0.90
	35	15.94	6.57	1.944	16.27	0.63

Effects of the initial diazinon concentration onto the adsorption process

The initial diazinon concentration had a parallel correlation with the rate of the adsorption process as shown in Figure 26. The initial diazinon increased from 5 $mg.L^{-1}$ to 35 $mg.L^{-1}$ caused the adsorption capacity of CC-BW, BG-BW, CF-BW increased from 1.78-8.60 $mg.g^{-1}$, 2.33-11.44 $mg.g^{-1}$, and 2.83-15.94 $mg.g^{-1}$, respectively. The result showed that increasing the diazinon concentration brought about the increase in adsorption efficiency. This is assumed that a higher adsorption capacity occurs when

increasing the initial diazinon concentration. This is because of increasing the initial diazinon concentration can cause the driving force of the concentration gradient was strengthened (66). This contrasted with the relationship between the initial diazinon concentrations and the adsorption rate constant of the PSO model. Table 10 demonstrated the adsorption rate constant k_2 (PSO) of diazinon at the lowest concentration was faster than the other concentrations and ratified with the previous work (66) too. The high initial concentration was the reason that causes a low rate constant k_2 (PSO) and vice versa. Moreover, from the data above showed that the adsorption capacity of CF-BW is higher than another two bio-wastes.

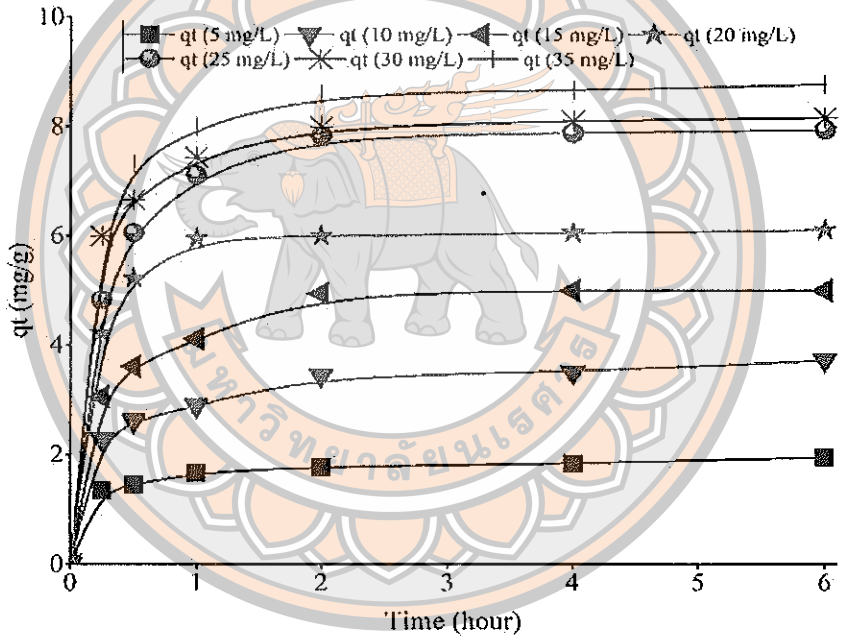

(a)

Figure 34 The adsorption capacities of diazinon by bio-wastes (a) CC-BW, (b) BG-BW, (c) CF-BW (The dosage of adsorbents = 1.5 $g.L^{-1}$, pH = 4)

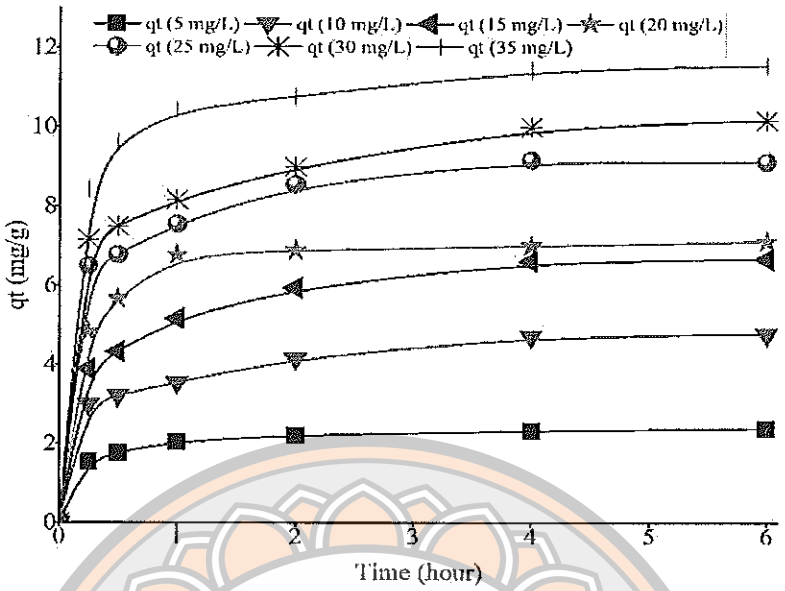

(b)

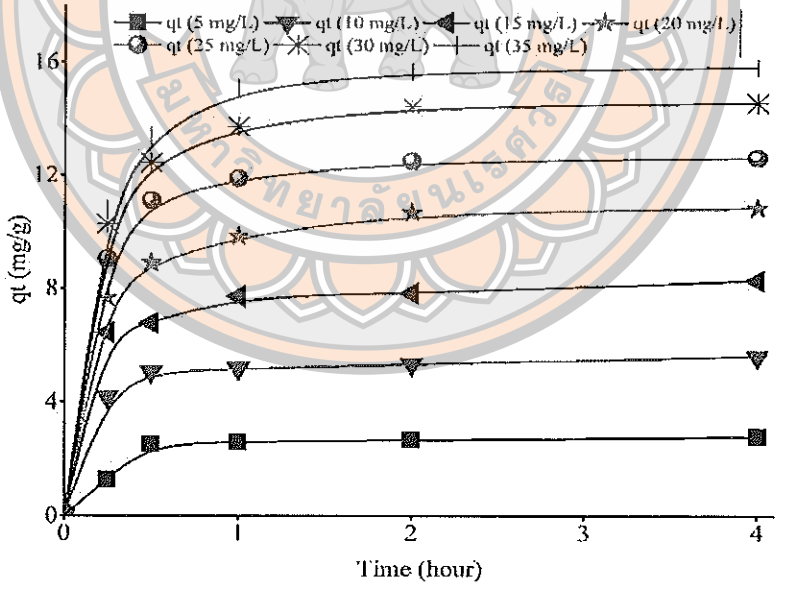

(c)

Figure 35 The adsorption capacities of diazinon by bio-wastes (a) CC-BW, (b) BG-BW, (c) CF-BW (The dosage of adsorbents = 1.5 $g.L^{-1}$, pH = 4)

CHAPTER V

CONCLUSION

This study examined the adsorption mechanism of bio-wastes for diazinon removal. Three types of bio-waste were derived from agro-waste, synthesized as a potential absorbent for diazinon removal from the aqueous environment. The synthesized condition is under the same pyrolysis conditions and modified with HF to enhance the specific area and porosity. Bio-wastes were synthesized for 4 h at a temperature of 600 °C.

pH 4 was the optimum pH of the solution that engendered the highest removal of diazinon. The specific surface area (BET) of CF-BW is higher than CC-BW and BG-BW in the ordering value 402.43 $m^2.g^{-1}$, 292.92 $m^2.g^{-1}$, and 67.42 $m^2.g^{-1}$, respectively. Likewise, the total pore volume of CF-BW is also higher than other bio-wastes by distribution into four sizes including, micropores (<2 nm), narrow mesopores (2-20 nm), mesopores (21-50 nm), and macropores (>50 nm). The pore volume disseminations in the size of the micropores (<2 nm) and narrow mesopores (2-20 nm) of bio-wastes in the range of 16.88-21.24 % and 56.57-69.22 %, respectively.

The adsorption isotherm of diazinon and three types of bio-waste was followed by the Langmuir isotherm model. The adsorption kinetics data of diazinon and the bio-wastes were fitted into the pseudo-second-order model. The adsorption capacity depended on the specific surface area and the total pore volume of the bio-waste. When the initial diazinon concentration was increased, this enhanced the adsorption capacity of bio-wastes. The pore-filling adsorption and the chemical interaction were the main factors in the adsorption mechanism. The chemical interaction included H-bonding, hydrophobic, and the π-π EDA interactions; however, the main contributor was H-bonding.

Overall, bio-wastes were very useful materials and had a high potential to contribute to the treatment of environmental pollutants.

REFERENCES

REFERENCES

1. Satish GP, Ashokrao DM, Arun SK. Microbial degradation of pesticide: A review. African Journal of Microbiology Research. 2017;11: 992-1012.

2. Machado SC, Martins I. Risk assessment of occupational pesticide exposure: Use of endpoints and surrogates. Regul Toxicol Pharmacol. 2018;98:276-283.

3. Cengiz M, Certel M, Gocmen H. Residue contents of DDVP (Dichlorvos) and diazinon applied on cucumbers grown in greenhouses and their reduction by duration of a pre-harvest interval and post-harvest culinary applications. Food Chemistry. 2006;98:127-135.

4. Krol WJ, Arsenault TL, Pylypiw HM, Incorvia MJ. Reduction of Pesticide Residues on Produce by Rinsing. Journal of Agricultural and Food Chemistry. 2000;48:4666-4670.

5. Damalas CA, Eleftherohorinos IG. Pesticide exposure, safety issues, and risk assessment indicators. Int J Environ Res Public Health. 2011;8: 1402-19.

6. Alavanja MCR. Pesticides Use and Exposure Extensive Worldwide. Reviews on environmental health. 2009;24:303-309.

7. Vera R, Insa S, Fontas C, Antico E. A new extraction phase based on a polymer inclusion membrane for the detection of chlorpyrifos, diazinon and cyprodinil in natural water samples. Talanta. 2018;185:291-298.

8. Salman JM, Njoku VO, Hameed BH. Adsorption of pesticides from aqueous solution onto banana stalk activated carbon. Chemical Engineering Journal. 2011;174:41-48.

9. Tsai WT, Chen HR. Adsorption kinetics of herbicide paraquat in aqueous solution onto a low-cost adsorbent, swine-manure-derived biochar. International Journal of Environmental Science and Technology. 2013;10: 1349-1356.

10. Hernández AF, Parrón T, Tsatsakis AM, Requena M, Alarcón R, López-Guarnido O. Toxic effects of pesticide mixtures at a molecular level: Their relevance to human health. Toxicology. 2013;307:136-145.

11. Dehghani MH, Kamalian S, Shayeghi M, Yousefi M, Heidarinejad Z, Agarwal S, et al. High-performance removal of diazinon pesticide from water using multi-walled carbon nanotubes. Microchemical Journal. 2019;145:486-491.

12. Wang C, Shih Y. Degradation and detoxification of diazinon by sono-Fenton and sono-Fenton-like processes. Separation and Purification Technology. 2015; 140:6-12.

13. Tripathi RK. Virginia Department of Health, Division of Environmental Epidemiology;2011.

14. Lyon F. Some organophosphate insecticides and herbicides International Agency for Research on Cancer;2017.

15. Al Hattab MT, Ghaly AE. Disposal and Treatment Methods for Pesticide Containing Wastewaters: Critical Review and Comparative Analysis. Journal of Environmental Protection. 2012;03:431-453.

16. Narayanan N, Gupta S, V. T. Gajbhiye, K. M. Manjaiah, Optimization of isotherm models for pesticide sorption on biopolymer-nanoclay composite by error analysis. Chemosphere. 2017;173:502-511.

17. Saleh S, Kamarudin KB, Ghani WAK, Kheang LS. Removal of Organic Contaminant from Aqueous Solution Using Magnetic Biochar. Procedia Engineering. 2016;148:228-235.

18. Khorram MS, Lin D, Zhang Q, Zheng Y, Fang H, Yu Y. Effects of aging process on adsorption-desorption and bioavailability of fomesafen in an agricultural soil amended with rice hull biochar. J Environ Sci (China). 2017;56:180-191.

19. Yavari S, Malakahmad A, Sapari NB. Biochar efficiency in pesticides sorption as a function of production variables—a review. Environmental Science and Pollution Research. 2015;22:13824-13841.

20. Inyang M, Dickenson E. The potential role of biochar in the removal of organic and microbial contaminants from potable and reuse water: A review. Chemosphere. 2015;134:232-40.

21. Desbski B, Kania B. F, Kuryl T. Transformations of Diazinon, an organophosphate compound in the environment and poisoning by this compound. ECOLOGY-BRATISLAVA. 2007;26(1):68.

22. Oliveira FR, Patel AK, Jaisi DP, Adhikari S, Lu H, Khanal SK. Environmental application of biochar: Current status and perspectives. Bioresource Technology. 2017;246:110-122.

23. Ahmad M, Rajapaksha AU, Lim JE, Zhang M, Bolan N, Mohan D, et al. Biochar as a sorbent for contaminant management in soil and water: a review. Chemosphere. 2014;99:19-33.

24. Tan X, Liu Y, Zeng G, Wang X, Hu X, Gu Y, et al. Application of biochar for the removal of pollutants from aqueous solutions. Chemosphere. 2015;125:70-85.

25. Mukherjee A, Zimmerman AR, W. Harris, Surface chemistry variations among a series of laboratory-produced biochars. Geoderma. 2011;163:247-255.

26. Zhang P, Sun H, Yu L, Sun T. Adsorption and catalytic hydrolysis of carbaryl and atrazine on pig manure-derived biochars: impact of structural properties of biochars. J Hazard Mater. 2013;244-245:217-24.

27. Sun K, Ro K, Guo M, Novak J, Mashayekhi H, Xing B. Sorption of bisphenol A, 17alpha-ethinyl estradiol and phenanthrene on thermally and hydrothermally produced biochars. Bioresour Technol. 2011;102:5757-63.

28. Tran HN, You SJ, Hosseini-Bandegharaei A, Chao HP. Mistakes and inconsistencies regarding adsorption of contaminants from aqueous solutions: A critical review. Water Res. 2017;120:88-116.

29. Sun K, Jin J, Keiluweit M, Kleber M, Wang Z, Pan Z, et al. Polar and aliphatic domains regulate sorption of phthalic acid esters (PAEs) to biochars. Bioresource Technology.2012;118:120-127.

30. Herath I, Kumarathilaka P, Al-Wabel MI, Abduljabbar A, Ahmad M, Usman ARA, et al. Mechanistic modeling of glyphosate interaction with rice husk derived engineered biochar. Microporous and Mesoporous Materials, vol. 225, pp. 280-288, 2016/05/01/ 2016.

31. Das O, Sarmah AK, Bhattacharyya DA. Sustainable and resilient approach through biochar addition in wood polymer composites, Science of The Total Environment, vol. 512-513, pp. 326-336, 2015/04/15/ 2015.

32. Fang Q, Chen B, Lin Y, Guan Y. Aromatic and Hydrophobic Surfaces of Wood-derived Biochar Enhance Perchlorate Adsorption via Hydrogen Bonding to Oxygen-containing Organic Groups. Environmental Science & Technology. 2014;48:279-288.

33. Zhu D, Pignatello JJ. Characterization of Aromatic Compound Sorptive Interactions with Black Carbon (Charcoal) Assisted by Graphite as a Model, Environmental Science & Technology, vol. 39, pp. 2033-2041, 2005/04/01 2005.

34. Mayakaduwa SS, Vithanage M, Karunarathna A, Mohan D, Ok YS. Interface interactions between insecticide carbofuran and tea waste biochars produced at different pyrolysis temperatures. Chemical Speciation & Bioavailability. 2016;28:110-118.

35. Inyang M, Gao B, Zimmerman A, Zhang M, Chen H. Synthesis, characterization, and dye sorption ability of carbon nanotube–biochar nanocomposites. Chemical Engineering Journal. 2014:236:39-46.

36. Chen B, Zhou D, Zhu L. Transitional Adsorption and Partition of Nonpolar and Polar Aromatic Contaminants by Biochars of Pine Needles with Different Pyrolytic Temperatures. Environmental Science & Technology. 2008;42:5137-5143.

37. Bolis V. Fundamentals in adsorption at the solid-gas interface. Concepts and thermodynamics. In: Calorimetry and thermal methods in catalysis. Springer, Berlin, Heidelberg. 2013;3-50.

38. Chincholi P, Sagwekar C, Nagaria S, Kulkarni, Dhokpande S. Removal of dye by adsorption on various adsorbent: A review. Int. J. Sci. Eng. Technol Res. 2014;3:835-840.

39. Lakherwal D, Adsorption of heavy metals: a review. International journal of environmental research and development, 2014;4(1):41-48

40. Webb PA. Introduction to chemical adsorption analytical techniques and their applications to catalysis. Micromeritics Instrument Corp. Technical Publications;2003.

41. Dada AO, Olalekan AP, Olatunya AM, DADA O. Langmuir, Freundlich, Temkin and Dubinin–Radushkevich isotherms studies of equilibrium sorption of Zn2+ unto phosphoric acid modified rice husk. IOSR Journal of Applied Chemistry. 2012;3(1):38-45.

42. Liu N, Zhu M, Wang H, Ma H. Adsorption characteristics of Direct Red 23 from aqueous solution by biochar. Journal of Molecular Liquids. 2016;223:335-342.

43. Tan G, Sun W, Xu Y, Wang H, Xu N. Sorption of mercury (II) and atrazine by biochar, modified biochars and biochar based activated carbon in aqueous solution. Bioresource technology. 2016;211:727-735.

44. Uchimiya M, Wartelle LH, Boddu VM. Sorption of triazine and organophosphorus pesticides on soil and biochar. Journal of agricultural and food chemistry. 2012;60(12):2989-2997.

45. An Q. Binh, Mechanism and kinetic study of pesticide removal by adsrption process using biochar. Doctor of phylosophy, Environmental Engineering, Naresuan University, 2018.

46. Wang L, Yan W, He C, Wen H, Cai Z, Wang Z, et al. Microwave-assisted preparation of nitrogen-doped biochars by ammonium acetate activation for adsorption of acid red 18. Applied Surface Science. 2018;433: 222-231.

47. Tran HN, Wang YF, You SJ, Chao HP. Insights into the mechanism of cationic dye adsorption on activated charcoal: the importance of π–π interactions. Process Safety and Environmental Protection. 2017;107: 168-180.

48. Chun Y, Sheng G, Chiou CT, Xing B. Compositions and sorptive properties of crop residue-derived chars. Environmental science & technology. 2004;38(17):4649-4655.

49. Saffari M, Karimian N, Ronaghi A, Yasrebi JR. Stabilization of nickel in a contaminated calcareous soil amended with low-cost amendments. Journal of soil science and plant nutrition. 2015;15(4):896-913.

50. Liu N, Charrua AB, Weng CH, Yuan XF. Ding, Characterization of biochars derived from agriculture wastes and their adsorptive removal of atrazine from aqueous solution: A comparative study. Bioresource technology. 2015;198:55-62.

51. Nuithitikul K, Srikhun S, Hirunpraditkoon S. Kinetics and equilibrium adsorption of Basic Green 4 dye on activated carbon derived from durian peel: Effects of pyrolysis and post-treatment conditions. Journal of the Taiwan Institute of Chemical Engineers. 2010;41(5):591-598.

52. Kinney TJ, Masiello CA, Dugan B, Hockaday WC, Dean MR, Zygourakis K, et al. Hydrologic properties of biochars produced at different temperatures. Biomass and Bioenergy. 2012;41:34-43.

53. Lian F, Cui G, Liu Z, Duo L, Zhang G, Xing B. One-step synthesis of a novel N-doped microporous biochar derived from crop straws with high dye adsorption capacity. Journal of environmental management. 2016;176:61-68.

54. Qiu Y, Zheng Z, Zhou Z, Sheng GD. Effectiveness and mechanisms of dye adsorption on a straw-based biochar. Bioresource technology. 2009; 100(21):5348-5351.

55. Liao Q, Sun J, Gao L. The adsorption of resorcinol from water using multi-walled carbon nanotubes. Colloids and Surfaces A: Physicochemical and Engineering Aspects. 2008;312(2-3):160-165.

56. Essandoh M, Wolgemuth D, Pittman CU, Mohan D, Mlsna T. Phenoxy herbicide removal from aqueous solutions using fast pyrolysis switchgrass biochar. Chemosphere. 2017;174:49-57.

57. Zheng H, Zhang Q, Liu G, Luo X, Li F, Zhang Y, et al. Characteristics and mechanisms of chlorpyrifos and chlorpyrifos-methyl adsorption onto biochars: Influence of deashing and low molecular weight organic acid (LMWOA) aging and co-existence. Science of The Total Environment. 2019; 657:953-962.

58. Olivella MA, Bazzicalupi C, Bianchi A, Fiol N, Villaescusa I. New insights into the interactions between cork chemical components and pesticides. The contribution of pi-pi interactions, hydrogen bonding and hydrophobic effect. Chemosphere. 2015;119:863-870.

59. Dehghani MH, Niasar ZS, Mehrnia MR, Shayeghi M, Al-Ghouti MA, Heibati B, et al. Optimizing the removal of organophosphorus pesticide malathion from water using multi-walled carbon nanotubes. Chemical Engineering Journal. 2017;310:22-32.

60. Dehghani MH, Fadaei A. Sonondegradation of organophosphorus pesticides in water. Environment Protection Engineering. 2013;39(4):5-14.

61. Hassan AF, Elhadidy H, Abdel-Mohsen AM. Adsorption and photocatalytic detoxification of diazinon using iron and nanotitania modified activated carbons. Journal of the Taiwan Institute of Chemical Engineers. 2017;75:299-306.

62. Teixido M, Pignatello JJ, Beltran JL, Granados M, Peccia J. Speciation of the ionizable antibiotic sulfamethazine on black carbon (biochar). Environmental science & technology. 2011;45(23):10020-10027.

63. Amani MA, Latifi AM, Tahvildari K, Karimian R. Removal of diazinon pesticide from aqueous solutions using MCM-41 type materials: isotherms, kinetics and thermodynamics. International journal of environmental science and technology. 2018;15(6):1301-1312.

64. Divband Hafshejani L, Hooshmand A, Naseri AA, Mohammadi AS, Abbasi F, Bhatnagar A. Removal of nitrate from aqueous solution by modified sugarcane bagasse biochar. Ecological Engineering. 2016;95:101-111.

65. Ho YS. Review of second-order models for adsorption systems. Journal of hazardous materials. 2006;136(3):681-689.

66. Weng CH, Lin YT, Tzeng TW. Removal of methylene blue from aqueous solution by adsorption onto pineapple leaf powder. Journal of hazardous materials. 2009;170(1):417-424.